WYLE LABORATORIES - RESEARCH STAFF

TECHNICAL MEMORANDUM 68-6

EXPERIMENTAL PROGRAM FOR THE INVESTIGATION OF TRANSONIC FLOW AROUND PROTUBERANCES IN THE AEDC-16T WIND TUNNEL FACILITY

WYLE LABORATORIES
TESTING DIVISION, HUNTSVILLE FACILITY

WYLE LABORATORIES - RESEARCH STAFF

TECHNICAL MEMORANDUM 68-6

EXPERIMENTAL PROGRAM FOR THE INVESTIGATION OF TRANSONIC FLOW AROUND PROTUBERANCES IN THE AEDC-16T WIND TUNNEL FACILITY

By

J.E. Robertson

Work Performed Under Contract NAS8-21026

May 1968

WYLE LABORATORIES
RESEARCH STAFF
Huntsville Facility Huntsville, Alabama

COPY NO. 37

TABLE OF CONTENTS

LIST OF FIGURES

LIST OF FIGURES (Continued)

LIST OF TABLES

1.0 INTRODUCTORY SUMMARY

For the past year, Wyle Laboratories have been engaged in a research program under Contract NAS8-21026 with NASA-MSFC to investigate the steady and unsteady aerodynamic characteristics of the flow around protuberances which extend into, and well beyond, attached turbulent boundary layers. The first task of this study was to conduct an extensive search of available literature for the purpose of accumulating data for a variety of protuberance geometries. Results of the literature survey indicated that considerable data were available for evaluating the mean flow around protuberances at superosnic speeds, with little data available on the fluctuating air loads which may be experienced in the vicinity of the protuberances. Further, there appeared to be a complete lack of both steady and unsteady aerodynamic data for protuberance flows at transonic speeds. This lack of transonic data poses a serious problem in the art of predicting steady and fluctuating air loads in the vicinity of protuberances for a launch vehicle, since, in the transonic flow regime, a launch vehicle experiences maximum dynamic pressure and, consequently maximum aerodynamic loads. However, for the study performed under the previous contract, some general features of protuberance flows were discovered (see Reference 1) and these features are summarized in the Technical Discussion, Section 2.0, of this report.

Following the survey and analysis of the data from published literature, a small scale wind tunnel test program was planned and subsequently conducted in the MSFC 14 by 14-inch Transonic Wind Tunnel. This test was conducted with three primary objectives. The first objective was to investigate general features of protuberance flows at transonic speeds using generalized protuberance geometries. Right circular cylinders of various heights and diameters which project into the flow with axes normal to the flow direction were selected for this study. The test was recently completed and the results are currently being analyzed. These data will be compared with supersonic data for similar protuberances to define similarities in the protuberance flow fields for the two Mach number ranges. The second objective of the small scale test was to investigate similarities between the flow fields for generalized protuberances and the flow fields for protuberances with specific geometries. For this phase of the study, models of the reaction control system (RCS) and the auxiliary propulsion system (APS) on the Saturn V were tested at the same conditions as for the generalized protuberance study. The third objective was to obtain base data that could be used to plan a large scale investigation of protuberance flows. At best, the small scale test results will reveal only qualitative information of the protuberance flow fields due to the limitations imposed by the model size on instrumentation density and measurement accuracy. This is particularly true for fluctuating pressure measurements because of the relatively large size of the microphones.

A large scale wind tunnel test is planned to obtain more detailed static and fluctuating pressure measurements for protuberance flows. For this test the use of an

existing model of the same general design as that tested in the small scale study, but of considerably larger scale is planned. This model has been modified for the purpose of the present study. The test will be conducted in the Propulsion Wind Tunnel, Transonic (16T) at the Arnold Engineering Development Center (AEDC), Arnold Air Force Station, Tennessee. A comprehensive outline of the test plan is presented in Section 2.3 of the Technical Discussion. This report was prepared in compliance with the requirements for a pre-test report set forth in Reference 2.

2.0 TECHNICAL DISCUSSION

2.1 Introduction

Protuberances have an infinite number of possible geometries so that a general discussion of the flow field is difficult. For example, the Saturn V alone has approximately 75 individual protuberances which include reaction control rockets, auxiliary propulsion systems, vents, tunnels, etc. (Reference 3.) Each protuberance generates its own flow field which may interact with the external flow field already present and lead to the imposition of large steady and fluctuating loads on both the protuberance and the surrounding structure. It is obviously impractical to investigate the environment of every protuberance which may be attached to the external surface of a launch vehicle, especially if some general features of the flow can be defined from a systematic study involving generalized protuberance geometries. In view of the free interaction hypothesis first advanced by Chapman, Kuehn, and Larson (Reference 4), it appears that the use of generalized protuberance shapes is a reasonable approach in studying protuberance flow fields. Essentially, they suggest that boundary layers undergo separation in a manner which is independent of the original cause. The separation commences well ahead of the protuberance, so that it is reasonable to suppose that the flow near the separation point is unaffected by the detail geometry of the protuberance. This phenomena has been proven in experiments for two-dimensional supersonic flow and is expected to apply to the three-dimensional case as well. However, even with this simplification, the flow close to the protuberance must be expected to be a function of the detailed protuberance shape. It follows that a definitive study of protuberance flow would involve measurements on the protuberance as well as on the structure which is in close proximity to the protuberance.

The planned wind tunnel test is based to some degree on the free interaction hypothesis discussed above. A basic detailed study will be conducted using cylindrical protuberances of various heights and diameters for which some mean flow data is now available. A basic reference length in the separated boundary layer generated by a protuberance is the undisturbed boundary layer thickness. Thus, protuberance height and diameter must be scaled with boundary layer thickness, and to accomplish this the test will include protuberances lying both within the well beyond the boundary layer. In addition, protuberances having more specific geometries will be tested and the results correlated with the clylindrical case. Specific protuberances of particular interest are the RCS and APS protuberances on the Saturn V.

The primary objective of the test is to determine the steady and fluctuating pressure characteristics of the protuberance flow field so that the environments of both the protuberance and the surrounding structure can be adequately defined. The protuberances will be mounted to a curved panel model which will be supported above the floor of the wind tunnel test section in a splitter-plate type installation. The

surface panel and certain protuberances will be instrumented with static pressure orifices and microphones to obtain the desired steady and fluctuating pressure measurements. Also, pitot pressure rakes will be installed in the surface panel to obtain boundary layer profile measurements. The protuberances will be tested over a range of Reynolds number (based on boundary layer thickness and protuberance diameters) and Mach number to determine the effect of these parameters or the protuberance flow fields.

2.2 Characteristics of the Mean Flow Around Protuberances

Any discussion of the mean flow around protuberances must be general, and for this reason, the discussion will be limited to the case of a cylindrical protuberance which projects into the flow with the axis of the protuberance normal to the flow direction. Details of separated turbulent flows generated by cylindrical protuberances at supersonic speeds are shown in Figure 1. The separation is accomplished by an oblique shock wave which extends downstream and intersects the bow shock of the cylinder. Below the point of intersection, the bow shock is deflected towards the cylinder forming the third leg of a lambda shock structure. The point of intersection is termed a triple point.

For cylindrical protuberances with height, in diameters, (H/D) greater than 1.5 and relative thin inflowing boundary layers (say $\delta/H \leq 0.25$), the flow field upstream of the protuberance may be divided into four regions: (1) the tip region located near the top of the protuberance, (2) the central region, (3) the triple point region and (4) the base region. The tip region is characterized by a curved bow shock which extends over the top of the protuberance. This region extends downward from the top of the cylinder for approximately 0.25 diameter. The central region extends from the tip region down to a point near the triple point. The oblique shock in three-dimensional flow would intersect the fylinder at $H/D \approx 1$ if there were no bow shock, so it may be assumed for practical purposes that the central region extends from the end of the tip region to a point where H/D is ≈ 1.0. In the central region the stagnation pressure on the cylinder is approximately constant and behaves as an infinite cylinder in cross flow (i.e., two-dimensional). The third region is the triple point region and may be assumed to be within $\pm (0.1) \cdot D$ of the triple point. This region may be viewed as a discontinuity in the flow and occurs because of the interaction of the three shocks. It is in this region that the peak pressure coefficient is found on the cylinder stagnation line and it is here that the maximum levels of fluctuating pressure may be anticipated. The fourth region is the base region where H/D goes from 0 to within 0.1 diameter of the triple point. This region may be subdivided into four flow zones; conical flow, separated shear layer flow, reverse flow and secondary flow. The conical flow zone is defined as the region of inviscid flow downstream of the oblique separation shock. The separated shear layer zone is one of turbulent flow formed by the separated boundary layer. The reverse flow zone is the region of low energy reverse flow encompassed by the separated shear layer. The secondary flow region near the root of the

cylinder consists of a substantially stagnant area where there is a small flow circumferentially around the protuberance. For cylinders with $H/D < 1.5$, the four regions tend to coalesce such that any one region is not clearly distinguishable from the other. Figure 2 is a three-dimensional sketch of the flow showing the geometry of the separation upstream of the cylinder.

For a given Mach number, the separation length in diameters (ℓ_s/D) was found to be a function of height for conditions where $H/D \leq 1.0$; whereas, for $H/D > 1.0$ the separation length was constant. Examples are presented for supersonic free-stream Mach numbers of 2.71 and 4.91 in Figure 3. For $H/D \leq 1.0$, the separation length and protuberance height are related by:

$$\frac{H}{D} = \frac{\ell_s}{D} \tan\theta + k, \quad H/D \leq 1.0 \qquad (1)$$

where θ is the oblique separation shock wave angle and k is a constant which is believed to depend on boundary layer thickness (δ). The accuracy of Equation 1 breaks down as H/D approaches zero, since for the limiting case of $H/D = 0$, deparation does not occur. Also, in the range of $0 < H/D < \delta/D$, the velocity is non-linear and the accuracy of Equation (1) is questionable. For most of the experimental results found in published literature, the angle of separation upstream of cylindrical protuberances was approximately 17 degrees. Assuming conical flow as suggested in Reference 1, the variation of shock wave angle (θ) with Mach number for a cone semi-vertex angle of 17 degrees may be determined fron conical flow charts. These data agree reasonably well with shock wave angles observed in a number of experiments as shown in Figure 4.

For high transonic Mach numbers ($1.0 < M_\infty \leq 1.6$). The oblique separation shock becomes approximately normal to the flow direction and the two-dimensional bow shock has a relatively large stand-off distance. For these conditions, the separation shock wave and the stand-off shock wave may be expected to coalese into a single shock with a loss in definition between the various flow regimes discussed above. Unfortunately, the only data taken in the range $1.0 < M_\infty \leq 1.6$ during the small scale test was at $M_\infty = 1.15$ and the accuracy of these data is questionable because of extraneous shock waves on the top surface of the test article. Therefore, any detailed discussion of the flow field at high transonic Mach numbers would be speculative.

2.3 Wind Tunnel Test Program

2.3.1 Objective and Scope

The present wind tunnel test program is the second of a two-part experimental investigation to define the steady and unsteady aerodynamic environments associated with the flow around protuberances at transonic speeds. The first-phase experiments involving small scale models have recently been completed and the results are presently in the reduction and analysis stage. In addition to providing basic data on the steady and fluctuating pressure characteristics of protuberance flow fields, the small scale results enabled optimum test specifications to be defined for the present test of large scale models. The primary objective of the present test is to define in detail the steady and fluctuating airloads on the protuberance and surrounding structure at transonic speeds. Both specific and generalized protuberance geometries will be investigated. Further, the effects of Reynolds number, boundary layer thickness, and Mach number will be defined.

2.3.2 Test Apparatus

Test Facility

The test will be conducted in the Propulsion Wind Tunnel, Transonic (16T) at AEDC. Tunnel 16T is a variable density wind tunnel with a 16 ft square test section. The walls of the test section are composed of perforated plates which allow continuous operation through the Mach number range from 0.55 to 1.60 with minimum wall interference. Details of the test section showing the model location are presented in Figure 5. A more estensive description of the tunnel is given in Reference 2 and the latest calibration results are presented in References 5 and 6.

Test Article

The basic test article will consist of a 30-degree segment of a cylindrical shell having a radius of curvature of 130 inches. The curved panel will be mounted in splitter-plate type fixture which will be supported above the tunnel floor (see Figure 5). An existing model (previously used for the pressure phase of the full scale Saturn V, S-IVB panel flutter test at AEDC) has been modified and will be used for the present test. Basic modifications consisted of replacing the existing corrugated surface panel with a smooth panel, and providing for the installation of instrumentation and protuberances together with their associated drive mechanisms. The protuberances and instrumentation will be mounted on a secondary panel (hereafter referred to as the test panel) which is 36.00 inches wide and 75.18 inches long and flush fitted into the basic panel structure (see Figure 6). The right hand side of the test panel (when viewed looking upstream) is attached to the basic structure through hinges which allow the test panel to be pivoted open and thus provides easy access to the instrumentation and protuberance drive system without

having to completely disassemble the test article. Also the instrumentation and drive system are attached to the test panel so that they are readily exposed when the model is open. This feature of the model design should greatly simplify model configuration changes, replacing of instrumentation, and the repair of mechanical systems in the event of damage. Further, this design concept will facilitate the model build-up since the basic structure can be installed in the test section cart concurrently with the installation of the instrumentation and the assembly of the protuberance drive mechanism. Protuberances for the basic study will be right cylinders of 2-4- and 8-inch diameter and will be telescoped into the flow over the test panel with the axes of the cylinders normal to the flow direction. Geometric details of the protuberances are shown in Figure 7. All of the protuberances will be raised and lowered with the same drive system. The drive system, shown in Figure 8, will enable the protuberances to be remotely raised and lowered to any height ranging up to 8 inches. Space limitations inside the splitter-plate limit the maximum travel of the drive system to 8-inches and since it is desirable to test all of the protuberances at heights ranging up to two diameters, it will be necessary to add an 8-inch extension to the basic 8-inch diameter protuberance for certain runs. In the fully retracted position, the top surface of all but the 8-inch diameter protuberance with the 8-inch extension will be flush with the test panel surface.

The drive system (Figure 8) consists of three jack screws and a lift plate to which the various cylindrical protuberances will be mounted. The drive system is supported between the underside of the test panel and a base plate by six support rods and two spacer bars. The jack screws are driven by a common 1/3 horsepower, 30 rpm electric motor through a chain and sprocket drive system. An O-ring seal is inserted in the test panel around the protuberance to seal the splitter-plate cavity from the top of the test panel and thus prevent leakage of air between the protuberance and test panel during the test.

Protuberance configuration changes are accomplished by removing the protuberance cap (see Figure 8) and detaching the base of the protuberance from the lift plate. Hole patterns in the lift plate provide for mounting all of the cylindrical protuberances on a common centerline as well as rotating the 8-inch diameter protuberance from 0- degrees to polar angles of 15- and 60- degrees (counter clockwise when viewed from the top). When the 8-inch diameter protuberance is rotated to 15- and 60- degrees, the protuberance cap remains at 0-degree orientation. That is, the cap is not rotated with the protuberance. For the 2- and 4-inch diameter protuberances, the gap between the test panel and the protuberance is filled with an instrumented insert panel. The insert panels attach to the test panel in the place of the removable ring (see Figure 8). O-ring seals similar to that used for the 8-inch diameter protuberance, are inserted between the insert panels and the smaller diameter protuberances to seal the gap.

In addition to the basic study, models of the RCS and APS protuberances on the Saturn V of approximately 20 percent scale will be tested (see Figure 9). These

models will be mounted to the same test panel used for the basic study, so that existing instrumentation can be utilized. For this phase of the test, the protuberance drive mechanisms will not be used.

A description of the various configurations is presented in Table I.

Instrumentation

Instrumentation in a given configuration of the test article will consist of a maximum of 296 static pressure orifices and 122 piezo-electric microphones which will be flush mounted in the test panel and the 8-inch diameter protuberance. The basic 8-inch diameter protuberance and the 8-inch diameter protuberance with the extension are the only protuberances that will contain instrumentation. Details of the instrumentation in the test panel, the insert panels and the 8-inch diameter protuberance configurations are shown in Figures 10, 11 and 12, respectively. The test panel will contain 216 static pressure orifices that are distributed in a polar array centered at the protuberance center (Model Station = 0), Figure 10a. The polar angles for the static pressure orifices are denoted by θ^+ and are measured in the clockwise direction when viewing the test panel from above. Most of the static pressure orifices are distributed along the centerline of the test panel (θ^+ = 0- and 180-degrees) and to the right side when viewed looking upstream. One ray of static pressure orifices are distributed at $\theta^+ = 270^\circ$ so that symmetry of the flow may be determined. The locations shown in Figure 10a are nominal dimensions and exact locations are presented in Table II. The identification symbols for the static pressure orifices are also presented in Table II. Also, the test panel will contain 107 microphones that will be distributed in a polar array along the panel centerline and to the left side of the test panel when viewed looking upstream. The polar angles for the microphones are denoted by θ^- and are measured in the counter-clockwise direction when viewing the test panel from above. This array of steady and fluctuating pressure instruments will provide optimum utilization of the instruments since the protuberance flow fields should be symmetrical about the panel centerline.

The insert panels that are used for the 2- and 4-inch diameter protuberances will contain static pressure orifices and microphones that are distributed in polar arrays similar to those of the test panel (see Figure 11). Each insert panel will contain 39 static pressure orifices and 15 microphones. Since the 2- and 4-inch diameter protuberances do not contain instrumentation, there will be a total of 255 active static pressure orifices and 122 active microphones for these two configurations. The total number of microphone channels that are available with the recorder system is limited to 122. Thus, microphone distributions in the insert panels are sparsely distributed and will provide only qualitative information of the unsteady pressure flow field in close proximity to cylindrical protuberances. However, detailed definition of the fluctuating pressure flow field near the cylindrical protuberances should be obtained for the 8-inch diameter protuberance which has a

relative high density of microphones in close proximity to the protuberance. The locations and identification symbols for the microphones in the test panel and insert panels are presented in Tables IV and V.

Both static and fluctuating pressure instruments will be located in the basic 8-inch diameter protuberance and the extension for this protuberance. Details of the instrument locations for the 8-inch diameter protuberance configurations are shown in Figure 12. The basic 8-inch diameter protuberance will contain 24 static pressure orifices and 6 microphones distributed at polar angles of 0, 30 and 120 degrees in the wall of the protuberance and 32 static pressure orifices and 9 microphones distributed in a polar array in the protuberance cap. Thus, for this configuration, there will be a total of 272 active static pressure orifices and 122 active microphones. For the 8-inch diameter protuberance configuration with the extension there will be 48 static pressure orifices and 15 microphones distributed at polar angles of 0-, 30- and 120 degrees in the wall of the protuberance. All the microphones for this configuration will be located in the walls of the extension portion of the protuberance with the base of the protuberance and the protuberance cap containing only static pressure instrumentation. The protuberance cap will contain 32 static pressure orifices as for the case of the basic 8-inch diameter protuberance configuration. Thus, for the 8-inch diameter protuberance configuration with the extension there will be a total of 296 active, static pressure orifices and 122 active microphones. The locations and identification symbols for the static pressure orifices and microphones in the 8-inch diameter protuberance configurations are presented in Tables VI and VII. Both 8-inch diameter protuberance configurations will be rotated about the centerline from 0-degrees to polar angles of 15- and 60- degrees such that static and fluctuating pressures will be recorded on the wall of the protuberances at polar angles of 0-, 15-, 30-, 45-, 60-, 90-, 120-, 165-, and 180- degrees. Because of the slight curvature of the protuberance cap, it will be necessary to maintain the cap at the 0-degree position. That is, the cap will not be rotated with the protuberance.

Other instrumentation on the test panel will consist of two pitot pressure rakes which will extend through the boundary layer for measurement of the boundary layer velocity profiles. Details of the rakes are shown in Figure 13. The forward rake will be remotely controlled so that it may be extended and retracted as desired during the test. This rake is designed such that, when in the fully retracted position, the top surface of the test panel will remain smooth. Further, this rake contains 15 pitot pressure probes distributed above the centerline of the test panel as denoted in Figure 13. In the extended position, the leading edge of the probes will be located 31.06 inches upstream of the protuberance center (modal station = 31.06.) The pressure for the static orifice in the test panel immediately aft of the forward rake will be recorded with the rake in the retarded position, and will be used together with the pitot pressure in the computation of the boundary layer velocity profiles in the upstream vicinity of the test panel. The aft rake is a fixed device and will be present throughout the test. The aft rake contains 25 pitot pressure

probes which are distributed above the panel centerline as shown in Figure 13. The upstream edge of the probes for this rake is located at model station 36.50. The pressure for the most aft static orifice in the test panel will be used in conjunction with the pitot pressures to compute the boundary layer velocity profiles for the aft region of the test panel. The pitot probe locations and identification symbols for the rakes are presented in Tables II and III.

A pitot-static probe will be extended into the secondary flow between the splitter-plate and the tunnel floor to monitor the flow in this region. The previous small scale test indicated that the secondary flow may be partially blocked at Mach numbers near 1.0. By monitoring the pitot-static probe beneath the splitter-plate and the boundary layer rakes above the test panel, the effect of any flow spillage over the leading edge of the model should be readily determinable. The static and total pressures (forward rake only) will be connected to a system of pressure scanning switches (Scani-valves) which will be mounted to the underside of the test panel. A total of ten- 48 port Scani-valves will be used to record the pressures. A typical static pressure installation is shown in Figure 14a. The scani-valve and port assignments for the various pressure components are presented in Table II. The total pressures for the aft rake will be conditioned through the AEDC-PWT Precision Pressure Balance (P^2 B) system. This system, which is considered to be more accurate than the Scani-valve system, will also be used to compute a reference pressure which will be compared to its counterpart on each of the Scani-valves. The comparison pressure is assigned to port 44 of each Scani-valve. The outputs from the Scani-valve and the P^2 B systems will be reduced and tabulated on-line utilizing the AEDC-PWT digital computer facilities. Also, the static and total pressure parameters will be stored together with identification and test condition parameters, on 800 bpi, IBM compatible digital magnetic tape for post-test analyses.

The microphones (or pressure transducers) recommended to be used for this test are the Kistler 601L quartz pressure transducers. These microphones have a resonant frequency of 130 Khz and previous calibrations conducted at NASA-MSFC indicate that frequency and phase are linear up to 20 Khz. The full scale pressure range is 300 psi and the active area of the diaphragm is 5/32-inch diameter. Kistler 553A charge amplifiers will be used to convert the quartz charge to a voltage signal. The charge amplifiers will limit the low frequency response to approximately 30 Hz. The amplifiers will also be housed inside the model. A typical microphone installation is shown in Figure 14b.

The Kistler pressure transducer systems will be calibrated in place by the use of a Photocon model PC-125 acoustic calibrator which has been modified so as to be hand held over each pressure transducer. Anticipated calibration levels are 150 dB and 160 dB (referenced to 0.0002 dynes per square centimeter) at 1 Khz.

The data acquisition system for the fluctuating pressure measurements will consist of the NASA-MSFC, 20 Khz constant bandwidth multiplexer and 14 track,

1.5 Mhz magnetic tape recorder. A block diagram of the system is shown in Figure 15. The multiplexer will provide close phase matching for data groups recorded on a single track and also will enable up to 122 data channels to be stacked on fourteen tracks. The data channels will be stacked 7 and 9 to a tape track with each channel having a 30 hz to 20-Khz frequency response. The microphone locations, identification symbols and track assignments are presented in Table IV. To provide for cross-correlating between data recorded on different tape tracks, it will be necessary to record a crystal oscillator signal and a wide-band white noise signal on all channels at the beginning of each reel of tape since phase matching across tape tracks is limited by the alignment of the tape recorder heads and tape skew. Also, the output from the crystal oscillator will be used in conjunction with a reference modulator to correct for tape speed errors. These signals will be recorded continuously with the microphone data during the test. A complete system calibration will be conducted immediately prior to the test and spot checked periodically during the test.

The vertical position of the various protuberances will be measured by a linear potentiometer which will be housed inside the model. The output from the potentiometer will be conditioned through the AEDC-PWT force and moment readout system (FAMROS) and subsequently reduced and tabulated on-line. Calibration of this instrument will also be required prior to the start of the test.

2.3.3 Test Description

Test Condition

Basic tests of all the configurations will be conducted in the Mach number range from 0.60 to 1.60 and at a constant Reynolds number of 3 by 10^6 per foot. This unit Reynolds number is near the maximum that can be held constant in Tunnel 16T for the specified Mach number range. The small scale test in the MSFC 14 by 14 inch Trisonic wind tunnel indicated that at $M_\infty = 0.80$ and 0.90 the flow was separated at the leading edge of the model which resulted in an unusually thick boundary layer over the top surface of the model. The model support system for that test was somewhat different from the support system for the current test; however, if similar poor flow is obtained during the present study, only the 8-inch diameter protuberance will be tested in the Mach number range associated with the poor flow. The effect of variation in Reynolds number will be investigated for all configurations if time permits. The order of priority for testing the various configurations for Reynolds number effects will be established during the test and will depend on the flow quality over the model experienced at subsonic Mach numbers. A similar status will apply for testing with an artifically thickened boundary layer. For the latter runs, the boundary layer will be tripped near the leading edge of the model so that the effects of boundary layer thickness on the protuberance flow fields can be established. Flow visualization studies using an oil flow technique are planned near

the end of the test. The extent of this invesitgation will depend on the flow quality over the model and the availability of test time. Oil flow studies are time consuming because of the necessity to clean the model between runs. Thus, it is anticipated that only a few representative conditions will be investigated during this study. A preliminary run schedule for the test is presented in Table VI. Variations of unit Reynolds number and dynamic pressure with Mach number for the basic test runs are presented in Figure 16.

Test Procedure

For the cylindrical protuberances, the protuberance height will be varied with Mach number held constant for a given run. It is desirable to obtain data only for monotonic variations in protuberance height because of hysteresis effects associated with boundary layer separation. For at least one configuration, data will be obtained for both increasing and decreasing protuberance height variations so that hysteresis effects can be defined. Varying protuberance height while holding Mach number constant will be faster than holding the height constant and varying Mach number because of the lesser time involved in raising and lowering the protuberances. However, for the 8-inch diameter protuberance with the extension, the drag load on the protuberance may be sufficiently large to necessitate minimum operation of the drive mechanism. Thus, for this configuration, protuberance height may be held constant and data obtained for monotonic variations in Mach number. The latter test procedure will be adopted for the RCS and APS protuberances since, for these configurations, protuberance height variations are not required.

Previous experience with the present instrumentation systems have indicated that noticeable instrumentation noise is generated by the operation of the Scani-valve drive systems which affect the microphone signals. Thus, static pressure data and microphone data will be obtained in sequential order rather than simultaneously. That is, for a given test condition the static pressure data will be recorded first, and when the acquisition of these data has cleared, the microphone outputs will then be recorded on magnetic tape. This procedure will also allow examination of the on-line tabulation of mean flow data prior to proceeding to new test conditions.

Data Reduction

It is necessary to perform a relatively extensive analysis of the measured data to define the basic characteristics of the inflowing attached turbulent boundary layer and the perturbed flow field around the protuberances. It is convenient to discuss the data reduction in terms of on-line and off-line requirements.

On-Line Requirements. In addition to the computation of standard test condition parameters, the on-line analysis will consist primarily of reducing the mean-flow parameters (static and total pressures) to descriptive terms. The static pressure measurements will be reduced to ratios of P/P_∞ and to standard coefficient form.

The total pressures from the boundary layer rakes will be reduced to ratios of velocity U/U_∞ and to local Mach number. The boundary layer displacement thickness and momentum thickness will also be computed from the total pressures at both the forward and aft rake positions as follows:

$$\delta^* = \int_0^{\delta} \left[1 - \frac{P_n}{P_{\bar{y}}} \frac{U_n}{U_{\bar{y}}} \right] dy \qquad (2)$$

$$\theta_B = \int_0^{\delta} \frac{P_n}{P_{\bar{y}}} \frac{U_n}{U_{\bar{y}}} \left[1 - \frac{U}{U_{\bar{y}}} \right] dy \qquad (3)$$

where

$$\frac{P_n}{P_{\bar{y}}} = \frac{\left(1 + 0.2\, M_n^2\right)^{-5/2}}{\left(1 + 0.2\, M_{\bar{y}}^2\right)^{-5/2}} \frac{P_{t_n}}{P_{t_{\bar{y}}}} \qquad (4)$$

$$\frac{U_n}{U_{\bar{y}}} = \frac{M_n}{M_{\bar{y}}} \sqrt{\frac{1 + 0.2\, M_{\bar{y}}^2}{1 + 0.2\, M_n^2}} \qquad (5)$$

M_n and P_{t_n} are the local Mach number and total pressure at pitot probe "n" respectively and $M_{\bar{y}}$ and $P_{t_{\bar{y}}}$ are the local Mach number and total pressure at the pitot probe corresponding to the maximum "y". For the forward rake, n = 1,2,3.....15, whereas for the aft rake, n = 1,2,3 ..... 25. Also, for the forward rake, $\bar{y}$ = 15, whereas for the aft rake, $\bar{y}$ = 25. The upper limit of integration in Equations (2) and (3), δ, is the boundary layer thickness and is equal to the "y" position for $U_n / U_{\bar{y}} \geq 0.99$.

The boundary layer displacement thickness and momentum thickness will also be computed at model station zero based on Bies' empirical relationships (Reference 16) as follows:

$$\delta^* = \frac{\left[1.3 + 0.43\, M_\infty^2\right] \delta}{10.4 + 0.5\, M_\infty^2 \left[1 + 2 \times 10^{-8}\, Re_x\right]^{1/3}}$$

$$\theta_B = \frac{\delta}{10.4 + 0.5\, M_\infty^2 \left[1 + 2 \times 10^{-8}\, Re_x\right]^{1/3}}$$

where $$\delta = 0.37\, X \left[Re_x\right]^{-1/5} \left\{ 1 + \left[\frac{Re_x}{6.9 \times 10^7}\right]^2 \right\}^{1/10}$$

X is the distance in feet from transition to model station zero. (For the purposes of these calculations, transition will be assumed to occur at the leading edge of the model.)

Re_x is the Reynolds number based on X.

Off-Line Requirements. Following the test, the static pressure results as stored on digital magnetic tape will be used to compute and plot both contour and surface plots of the mean flow pressure field around the various protuberances. A smooth surface, interpolation scheme will be applied to the measured pressures utilizing the MSFC - IBM 7094 computer and the plots will be generated by the MSFC-4020 plotter. The computer program for performing the mean flow analysis is in preparation by Wyle Laboratories personnel.

The microphone fluctuating pressure measurements, as recorded in multiplexed form on magnetic tape, will be reduced to descriptive statistical parameters after the test by digital techniques. The CDC-3300 digital computer and analog-to-digital data conversion system at Wyle Laboratories will be used for processing the microphone data. A description of the computing facilities and some of the computer programs presently available at Wyle Laboratories for processing stationary random data are outlined in Section 3.0. Certain of the programs will be modified to reduce the fluctuating pressure measurements to statistical parameters that are compatible with MSFC requirements.

The data reduction procedure for the fluctuating pressure measurements may be considered as composed of the following phases.

(i) conversion of continuously recorded multiplexed data to a demultiplexed digital form

(ii) calculation of overall level (RMS or dB)

(iii) calculation of power spectral densities

(iv) calculation of cross-spectral density functions

(v) calculation of coherence functions

In the analog-to-digital conversion phase, the first consideration is the sampling rate, h. The well-known Nyquist criterion requires

$$h \geq 2f_n$$

where h is in samples/second and f_n is the highest frequency present in the data in hertz. However, as a precaution to avoid analyzing data with high frequency noise it will be necessary to filter the data at frequencies above f_n. It is presently planned to analyze the data at frequencies up to 20 Khz.

The acquisition of the data in digital form will be carried out in the manner required by the cross-correlation phase, since it is desirable that pairs of channels which are to be cross-correlated be sampled simultaneously. An analog-to-digital conversion program similar to RANDAQ (Section 3.2.1) will be used for this phase.

Overall levels may be calculated directly from the sampled data or obtained indirectly from the power spectral density calculations. It is proposed to use both methods so that cross-checking the two results may be used as a means of checking the power spectral density calculations. Power spectral densities may be calculated by programs similar to CONSTBWD or ANALYSIS. Program CONSTBWD calculates spectral density estimates for constant frequency bandwidths across the frequency range; whereas, program ANALYSIS produces selectively variable bandwidths which are constant in an octave band but doubling with each increasing octave. The method employed in both programs is that of calculating the autocorrelation function and then applying a Fourier Transform to the autocorrelation function. Parameters which are open to the choice of the user are the number N of data samples to be used and the number of lags m for which the autocorrelation is to be calculated. The choice of these parameters is important in the following two respects:

(i) The frequency interval for which power spectral density estimates are calculated is $h/2m$ and thus corresponds to an equivalent filter bandwidth of h/m hertz, i.e., two estimates are obtained per bandwidth.

(ii) The number of statistical degrees of freedom is given by $2N/m$, which represents the statistical sampling accuracy of the estimates. The result applies strictly only to band limited white noise and a spectrum with distinct peaks will have considerable less statistical stability than indicated above.

The relationship between the ratio of measured value to true value with statistical degrees of freedom for various confidence levels is known from theory. It is usual to use at least 100 for the number of degrees of freedom; bandwidth requirements are usually determined by the physical origin of the data. For the present analysis a one-third-octave analysis is planned.

An alternative method of calculating power spectral density, which has the advantage of a considerable saving of computer time over the method briefly described above, is that of a direct Fourier transformation of the original time series using the "Fast Fourier Transform" algorithm. The power spectral density is obtained at a particular frequency from the sum of the squares of the (complex) Fourier coefficients which have been smoothed using an appropriate spectral window.

In this method the time data is sectioned into a series of short records of length p and the spectra averaged over the sub-records. The bandwidth is $2h/p$ and the number of degrees of freedom is $2N/p$; the method is thus equivalent to the autocorrelation method with $p = 2m$, but has one-half the number of degrees of freedom for the same value of N. The restriction on this method is that p must be a power of 2 which means that the bandwidth choice is not as flexible as in the autocorrelation method. This also results in limitation in the form of the output available. However, experience with both methods at Wyle Laboratories has shown that the Fast Fourier Transform method to be faster than the autocorrelation/Fourier transform by a ratio of between 3 and 4 to 1 including graphical output of results. A computer program which implements the FFT method is being modified at Wyle Laboratories and will be used for calculating power spectral density in one-third-octave bands.

Cross-correlation may be calculated using the conventional lagged product method (as in computer program ANALYSIS, Section 3.2.3) or advantage may be taken of the FFT method whereby the cross-correlation is calculated from a Fourier transform of the cross spectral density. For the present analysis, only cross spectral density will be computed using the FFT method.

The remarks concerning statistical degrees of freedom made above apply equally to correlation functions and values of N and m will be chosen to meet a specified number of degrees of freedom. A further consideration in the choice of m is that it must be large enough to determine the highest peak in the correlation function. Program output will be in a form consistent with that currently in use at MSFC.

Wyle Laboratories' comprehensive three-dimensional plotting routines will also be used as required and could offer substantial simplification in the analysis of the results. Possible plots include overall level (in any frequency band if necessary) as a function of position over an area surrounding the model, frequency spectrum against a model parameter, simultaneous phase and amplitude plots for cross spectra, or any desired combinations of three variables.

3.0 COMPUTING FACILITIES

3.1 Introduction

Wyle Laboratories utilizes the Control Data Corporation's Huntsville Data Center which is capable of solving theoretical problems and processing analog data. The Data Center is located at Wyle-Huntsville.

The facility is designed around a Control Data Corporation 3300 Series digital computer, which is capable of high speed on-line analog data processing of experimental data. Thus, the facility is designed to support both research and environmental test programs, including those with on-line requirements.

Experimental data stored on magnetic tape is digitized by a synchronized dual-channel analog to digital conversion subsystem directly on-line to the Control Data Corporation 3300 computer system. The analog to digital converted data can be processed, analyzed, and reduced to engineering terms in a very short time to facilitate a rapid analysis of the data. All phases of the analysis can be done at the same time; i.e., auto-correlations, power spectra, cross-correlations, cross-power spectra and statistical distributions, can be obtained quickly and accurately.

The CDC 3300 digital computer system is capable of acquiring analog data and converting it to digital format over two simultaneous channels at a rate of 60,000 12 bit samples per second per channel. The converted data is recorded on digital magnetic tape continuously, keeping the above rates constant. Once all of the data is recorded, it is analyzed and reduced to printed form, graphical display, and/or punched cards.

The extremely high speed of the CDC 3300 system makes processing of large amounts of experimental data both feasible and economical. The capability of the system for scientific problem solving, which is virtually unlimited, is additionally supported by the most up-to-date scientific compiling (computer language translating) and system monitoring programs available.

The following is a description of the general purpose computer programs written by staff members and available at Wyle Laboratories for the calculation, from stationary, random data, of auto-correlation, cross-correlation, direct power spectral density, cross power spectral density and spatial correlation. All the programs discussed below are complete, however, modifications will be required to certain programs for the purpose of the present analysis.

3.2 Computer Programs for Reducing Stationary Random Data

3.2.1 Data Acquisition

Program: RANDAQ

Source Language: Machine (Assembly) Language

This program acquires the digitized data from the Analog/Digital input channels in real time and writes the data on a pair of magnetic tapes. Input may be from live tests or analog tapes. The input channels are divided between two multiplexers which are sampled simultaneously; channel groups may be sub-multiplexed to give various sampling rates.

The number of channels to be acquired, sampling rate, sub-multiplexed groups and number of data to be collected are determined by control cards read by the program.

3.2.2 Auto-correlation and PSD with Constant Bandwidth

Program: CONST BWD

Source Language: Machine (Assembly) Language

This program uses the data acquired by program RANDAQ to calculate auto-correlation and power spectral density with constant bandwidth by the mean lagged product method. Results are output on a digital incremental plotter.

The frequency range of the results is determined by the sampling rate and the bandwidth of the PSD estimates is specified by the number of lags required in calculating the auto-correlation function. The number of data values used, in conjunction with the number of lags, is chosen to keep the statistical degrees of freedom greater than 100. All these parameters are input parameters to the program with the restriction that the number of lage cannot exceed 3000.

3.2.3 Auto-correlation, Cross-correlation, Direct PSD and Cross-PSD with Selectively Variable Bandwidth

Under this heading there are three separate programs. The selective bandwidth feature is obtained by taking the original data and producing a series of new records by successively low pass digital filtering to remove half the frequency content and then discarding alternate points to double the effective sampling rate. PSD estimates are then obtained for various octaves with a constant bandwidth in each octave, but with the bandwidth double that of the previous lower octave.

Program: Filter

Source Language: Machine (Assembly) Language

This program takes a specified number of data acquired by RANDAQ and demultiplexes it into contiguous elements of a time series. Successive low pass filtering and "decimation" (discarding alternate points) with cut-off frequency half the maximum frequency of the data being filtered produces a time series for each octave in the frequency range. The results are output on magnetic tape; statistical quantities, such as mean, variance, standard deviation, skewness and kurtosis for the original time series are printed.

Program: ANALYSIS

Source Language: Machine (assembly) Language

The output of FILTER is used by this program to calculate auto- or cross-correlation by the mean lagged product method and direct or cross PSD by a Fourier transform of the correlations. These quantities are obtained for a specified number of octaves with a specified number of points to give a value of statistical degrees of freedom greater than 100 in the lowest octave. In each octave the frequency bandwidth is double that of the previous one, with the first bandwidth chosen by the sampling rate and number of lags. Output is to a magnetic tape for subsequent plotting but an option exists to have the results printed also.

Program: PLOTSBA

Source Language: Machine (Assembly) Language

This program plots the results of ANALYSIS on a digital incremental plotter. Options are available to include or suppress correlation plots. PSD plots are on a log-log grid.

3.2.4 Spatial Correlation

Program: SPACORR

Source Language: FORTRAN and Machine (Assembly) Language

This program uses the output of FILTER to calculate the spatial correlation between a pair of data series. Spatial correlation is determined in terms of cross- and direct spectral estimation and also uses the selective bandwidth technique described in 6.2.3. Output of results is to a printer but consideration is being given to a general plotting procedure. Development is also in progress in adapting the program to calculating auto- and cross-correlations using FFT.

3.2.5 Probability Density Function

Program: PROBDENF

Source Language: FORTRAN

This program takes the output of RANDAQ and for the specified channel number calculates the probability density function for it, plus other statistical data. The probability function is output as a graph on the printer and gives an immediate indication of the distribution of the time data (e.g., whether Gaussian or not, existence of a discrete frequency, peak clipping by the hardware, etc.)

Development is also in progress on a program to calculate the joint probability density function for a pair of time series.

4.0 REFERENCES

1. Dendrinos, S. Jr., "Prediction of Mean Flow Characteristics About Three-Dimensional Protuberances in Supersonic Flow," Wyle Laboratories Research Staff Report WR 67-19, November 1967.

2. Test Facilities Handbook (6th Edition), "Propulsion Wind Tunnel Facility Vol. 5," Arnold Engineering Development Center, November 1966.

3. Reich, J.R., "Saturn V External Protuberances, Cavities, and Corrugations," Lockheed Missiles and Space Company, Huntsville Technical Memorandum, TM-54/50-43, May 1966.

4. Chapman, D.R. Kuehn, D.M. and Larson, H.K., "Investigation of Separated Flows in Supersonic and Subsonic Streams With Emphasis on the Effects of Transition," NACA Rep. 1356.

5. Chevalier, H.L., "Calibration of the 16-Foot Transonic Circuit With a Modified Model Support System and Test Section," AEDC-TN-60-164, (AD 241 735), August 1960.

6. Riddle, C.D., "An Investigation of Free-Stream Fluctuating Pressures in the 16-Foot Tunnels of The Propulsion Wind Tunnel Facility, AEDC-TR-67-167, August 1967.

7. Voitenko, D.M. et al., "Supersonic Gas Flow Past a Cylindrical Protuberance on a Plate," AD 650 960, January 1967.

8. Halprin, R.W., "Study of the Separated Regions Caused by Two-Dimensional and Cylindrical Steps Mounted on a Flat Plate in a Supersonic Turbulent Flow," Master's Thesis, University of California, Los Angeles, 1964.

9. Couch, L.M. et al., "Heat Transfer Measurements on a Flat Plate with Attached Protuberances in a Turbulent Boundary Layer at Mach Numbers of 2.49, 3.51 and 4.44," NASA TN D-3736, December 1966.

10. Burbank, P.B. Strass, K.H., "Heat Transfer to Surfaces and Protuberances in a Supersonic Turbulent Boundary Layer," NACA RM L58E 1a, July 14, 1958.

11. Burbank, P.B. et al., "Heat Transfer and Pressure Measurements on a Flat-Plate Surface and Heat Transfer Measurements on Attached Protuberances in a Supersonic Turbulent Boundary Layer at Mach Numbers of 2.65, 3.51 and 4.4, NASA TN D-1372, December 1962.

12. Price, E.A. and Stalling, R.L. Jr., "Investigation of Turbulent Separated Flows in the Vicinity of Fin Type Protuberances at Supersonic Mach Numbers, NASA TN D-3804, February 1967.

13. Miller, W.H., "Pressure Distributions on Single and Tandem Cylinders Mounted on a Flat Plate in Mach Number 5.0 Flow," University of Texas Defense Research Laboratory Report 538, (N66-28598), June 1966.

14. Westkaemper, J.C., "The Drag of Cylinders All or Partially Immersed in a Turbulent Supersonic Boundary Layer," University of Texas Defense Research Laboratory Report 549, (AD 813 886), March 1967.

15. Ames Research Staff, "Equations, Tables, and Charts for Compressible Flow," NACA Report 1135, 1953.

16. Bies, D.A., "A Review of Flight and Wind Tunnel Measurements of Boundary Layer Pressure Fluctuations and Induced Structural Response, NASA CR-626, October 1966.

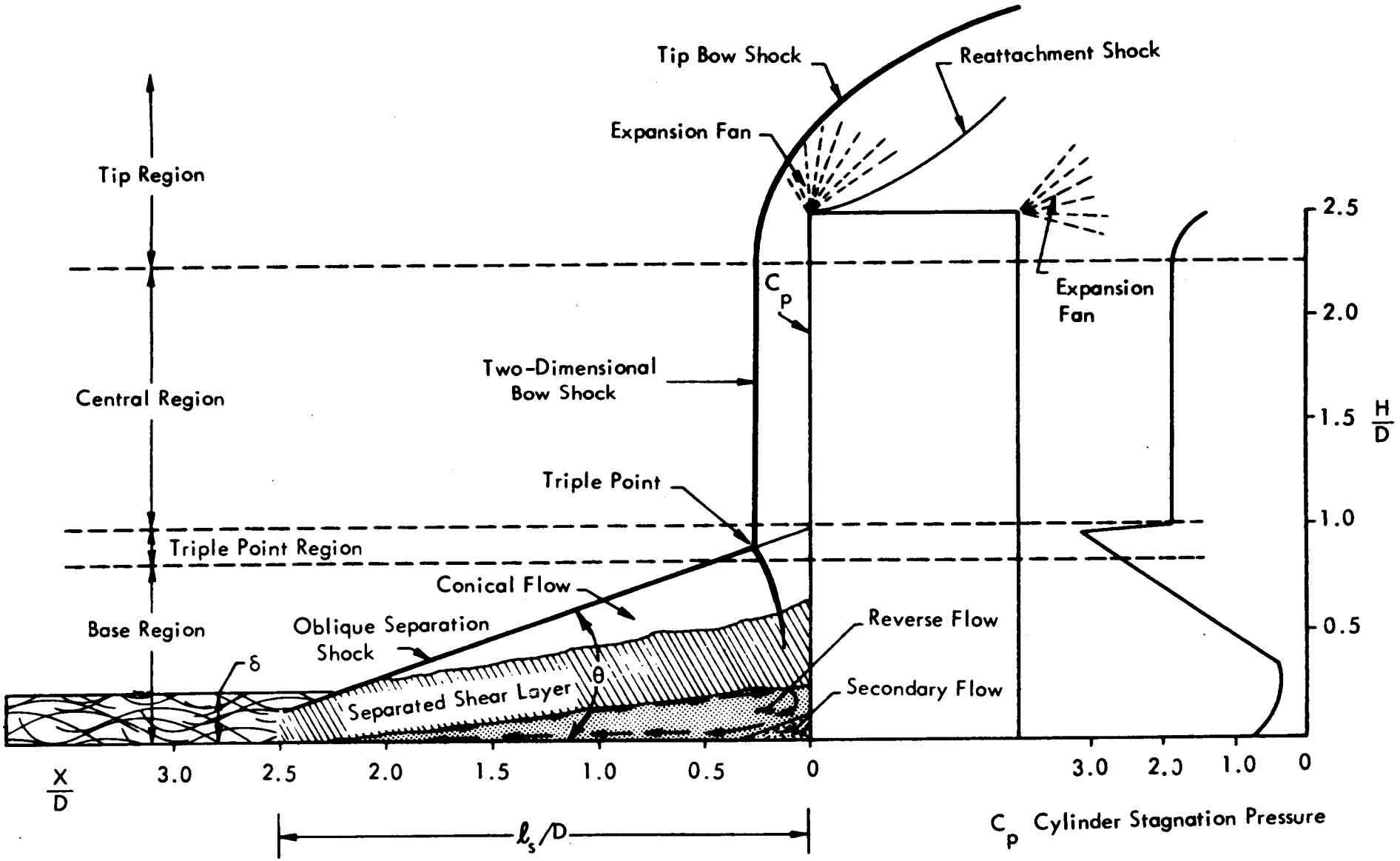

Figure 1. Characteristics of the Mean Flow Around a Cylindrical Protuberance (Reference 1)

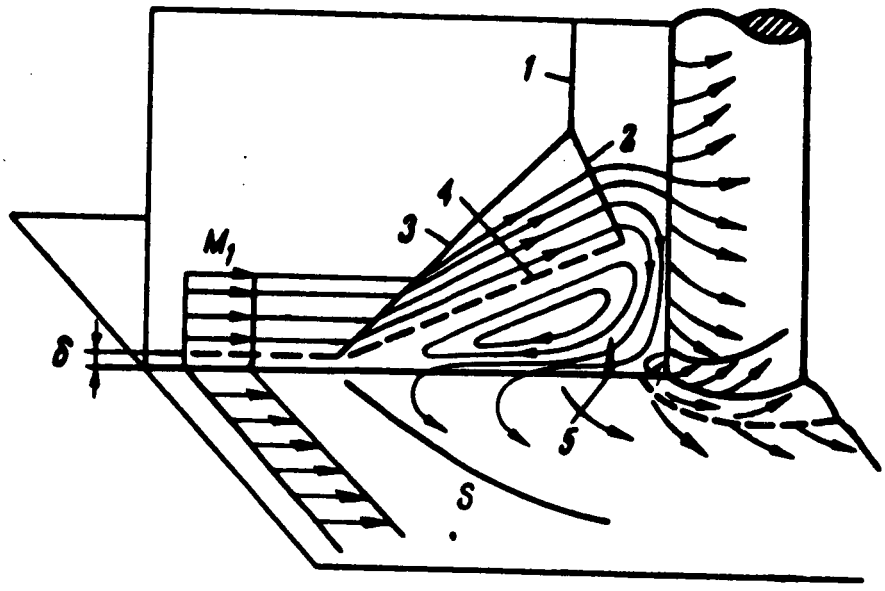

Voitenko et al
Reference 7

1. The detached shock wave
2. The shock wave ahead the cylinder
3. The oblique shock wave
4. The stagnation zone boundary
5. The minimum pressure region

Figure 2. Three-Dimensional Flow Pattern Around a Cylindrical Protuberance

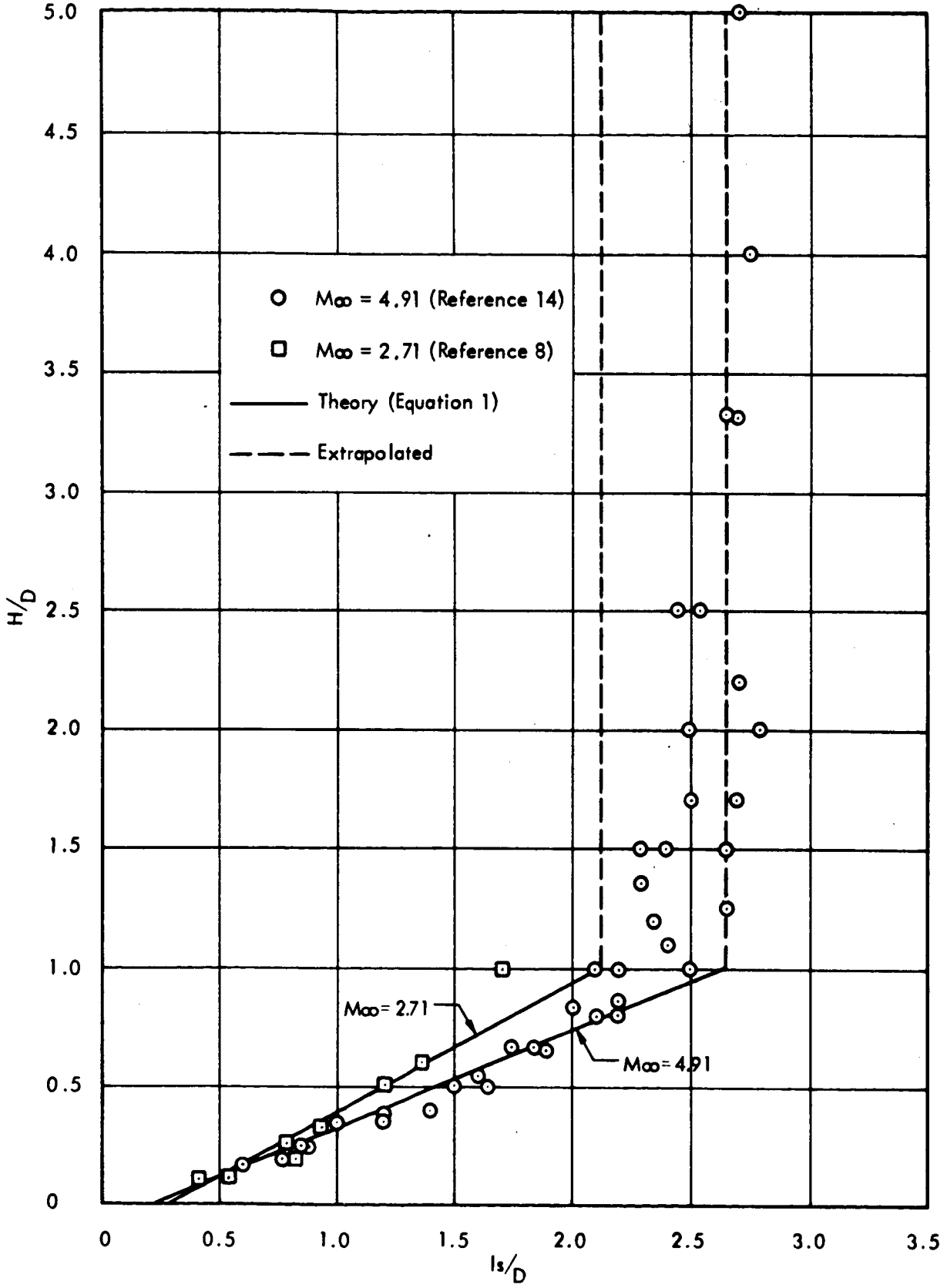

Figure 3. Effect of Normalized Height on Normalized Separation Length for Cylindrical Protuberance

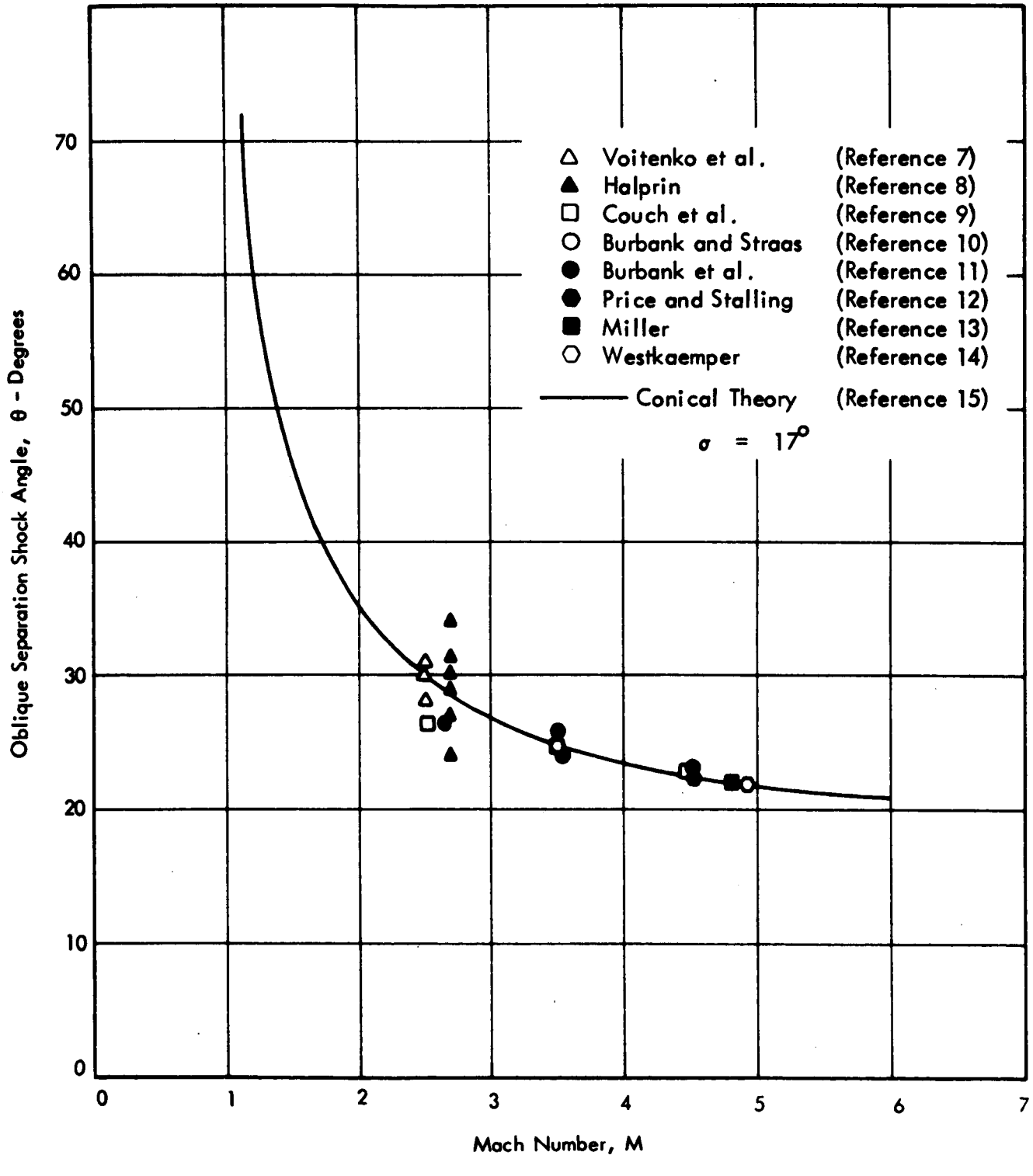

Figure 4. Variation of Oblique Separation Shock Angle with Mach Number

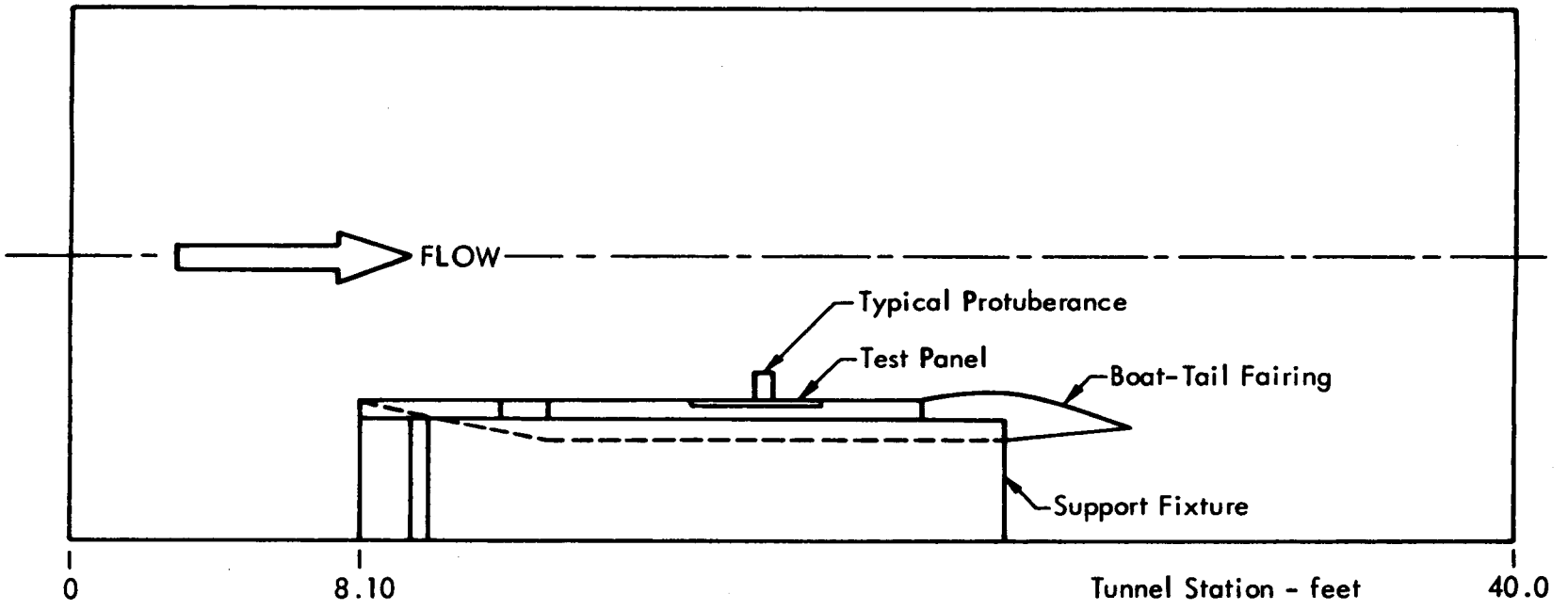

Figure 5. Schematic of the Test Article Installation in the AEDC - 16T Wind Tunnel Facility

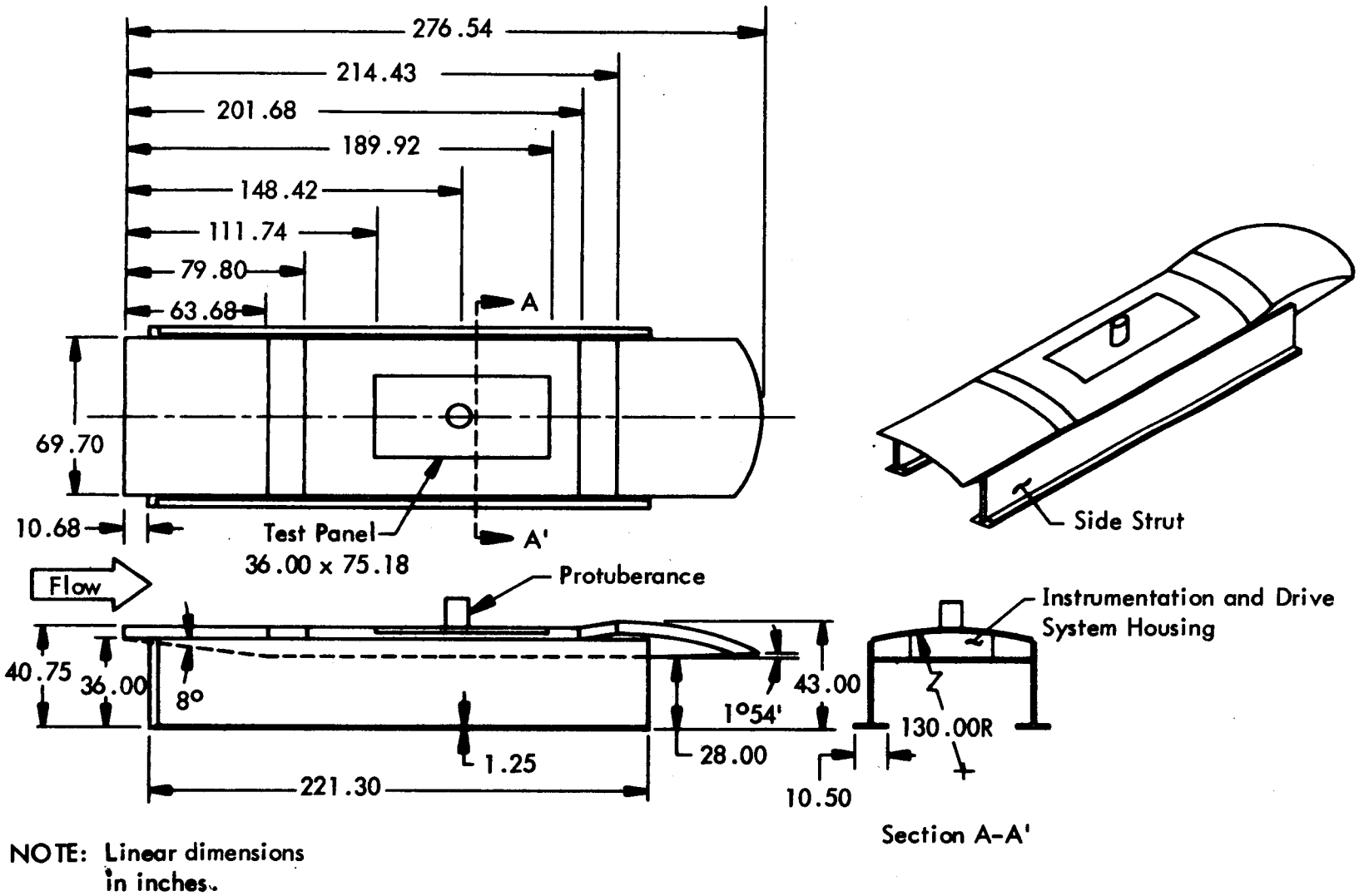

Figure 6. Details of the Test Article

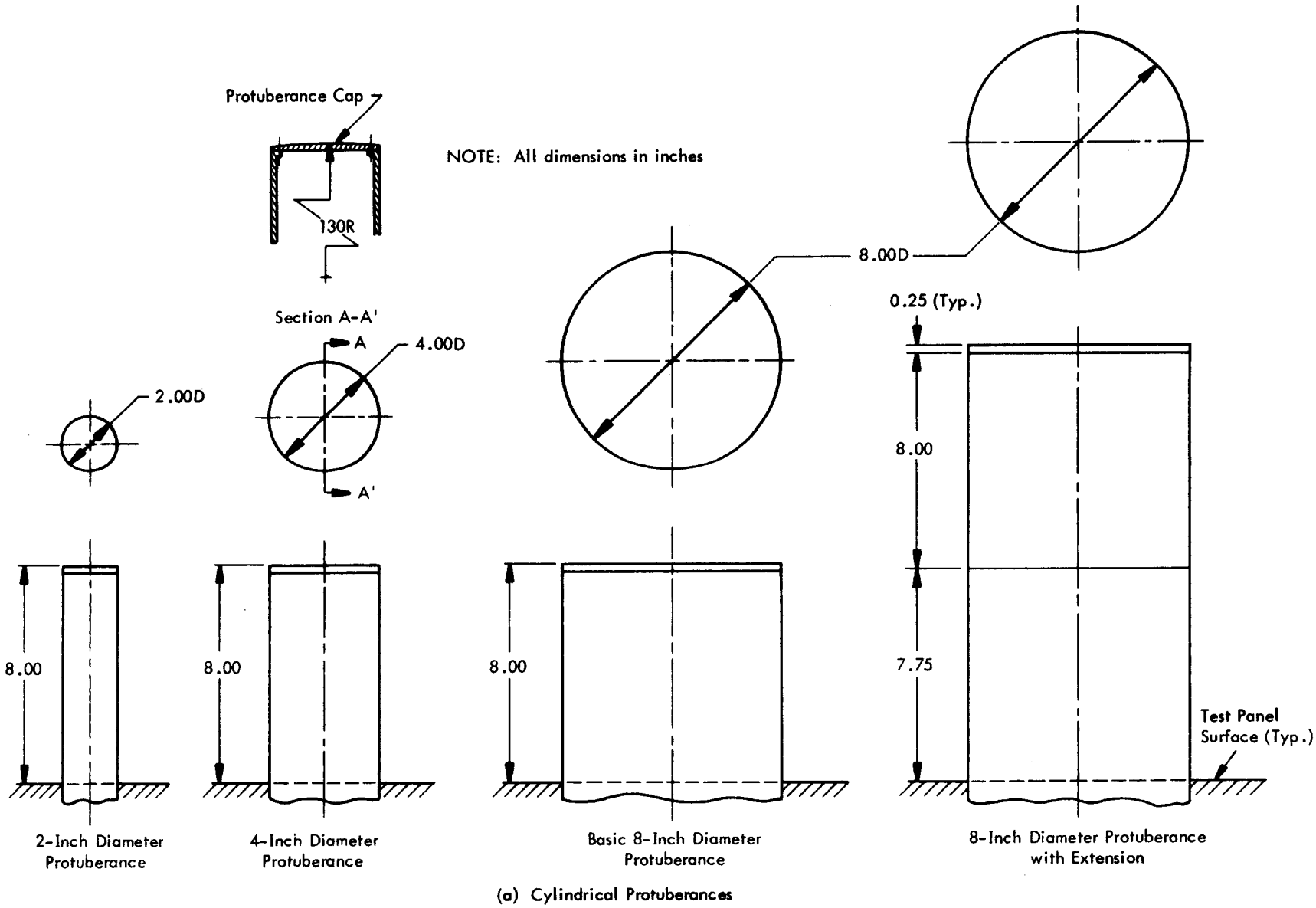

(a) Cylindrical Protuberances

Figure 7. Details of the Cylindrical Protuberances

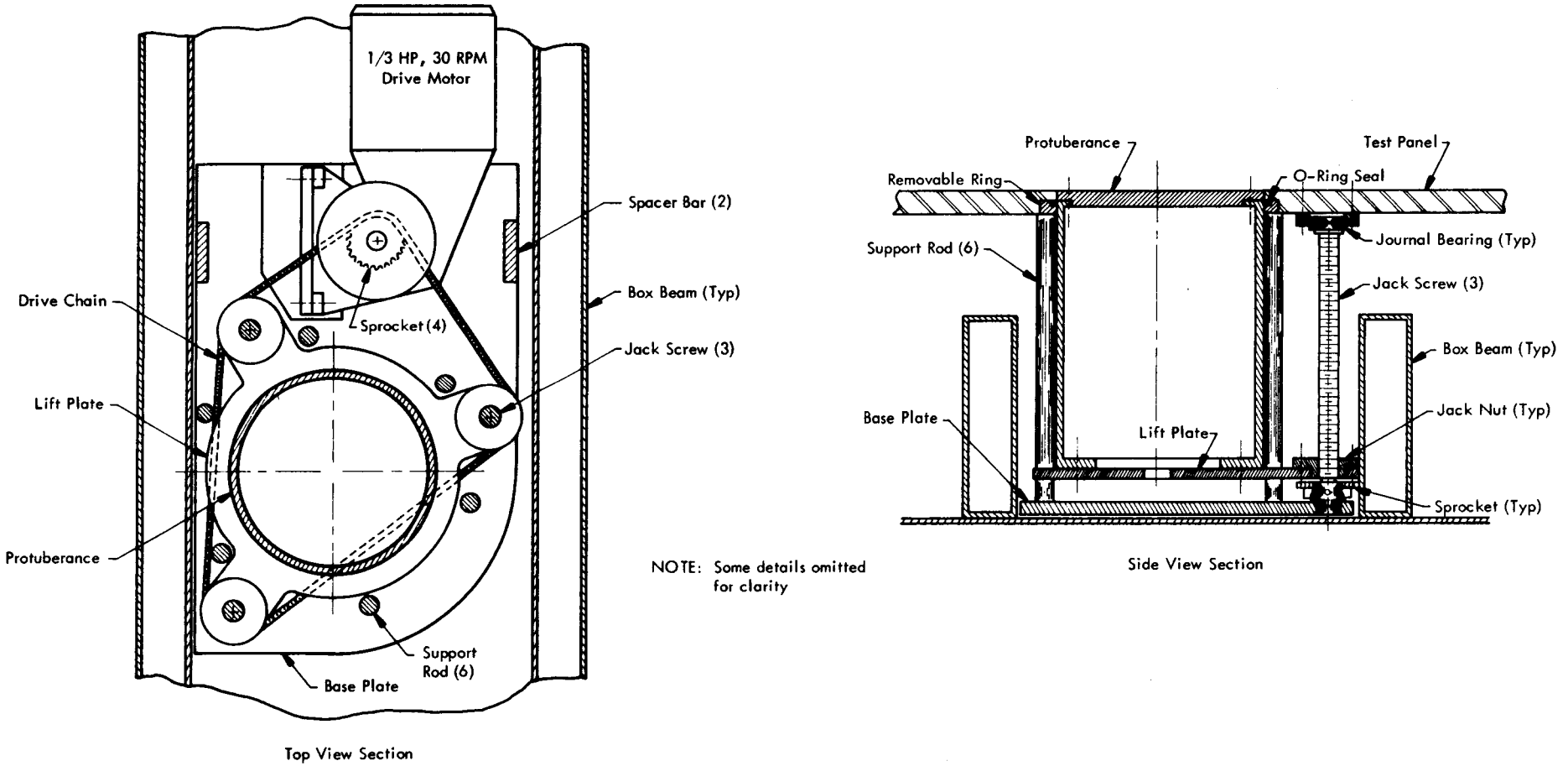

Figure 8. Details of the Cylindrical Protuberance Drive System

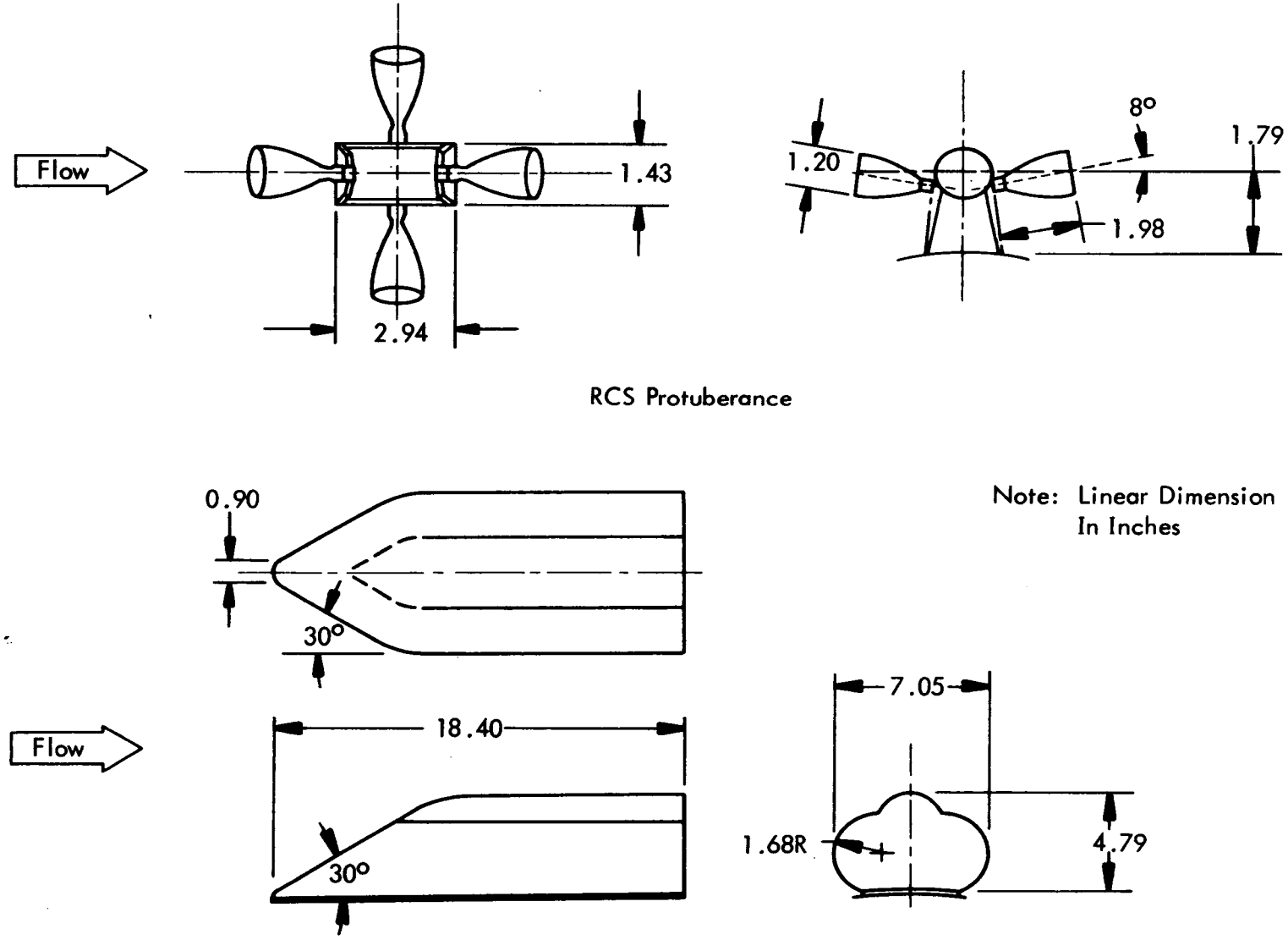

Figure 9. Details of the RCS and APS Model Protuberances

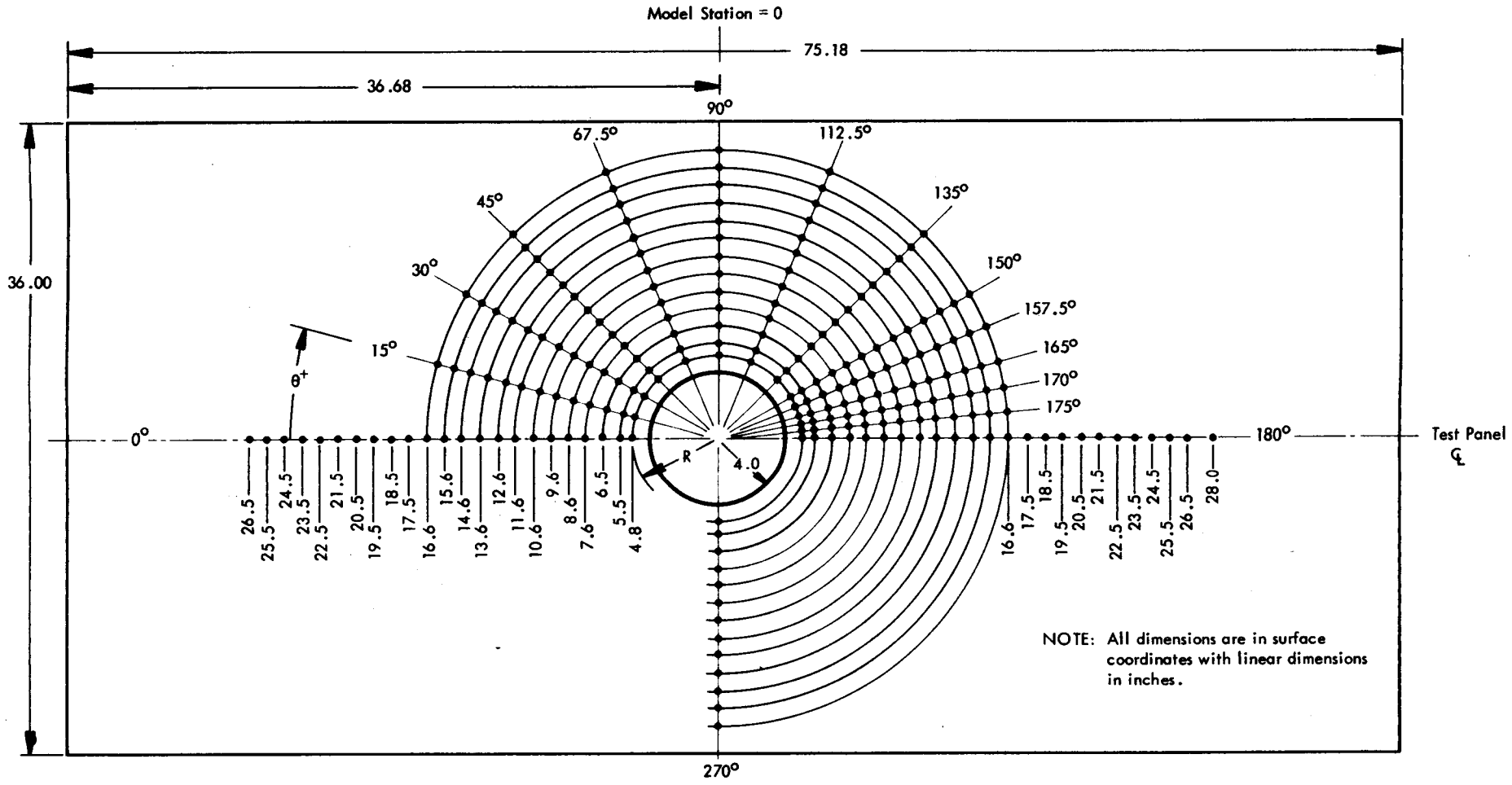

(a) Static Pressure Instrumentation

Figure 10. Instrumentation Location in the Test Panel

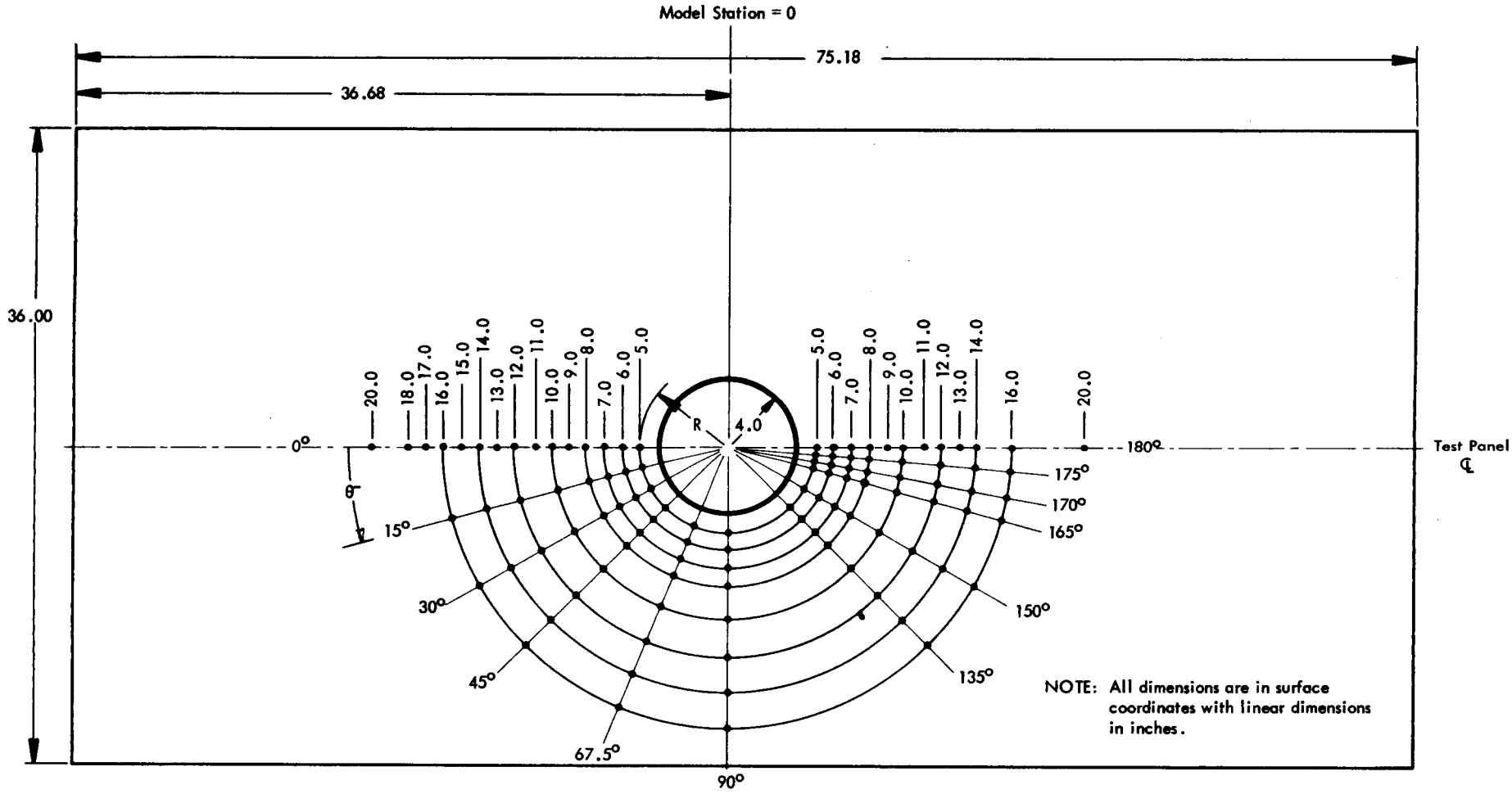

(b) Microphone Instrumentation

Figure 10. Concluded

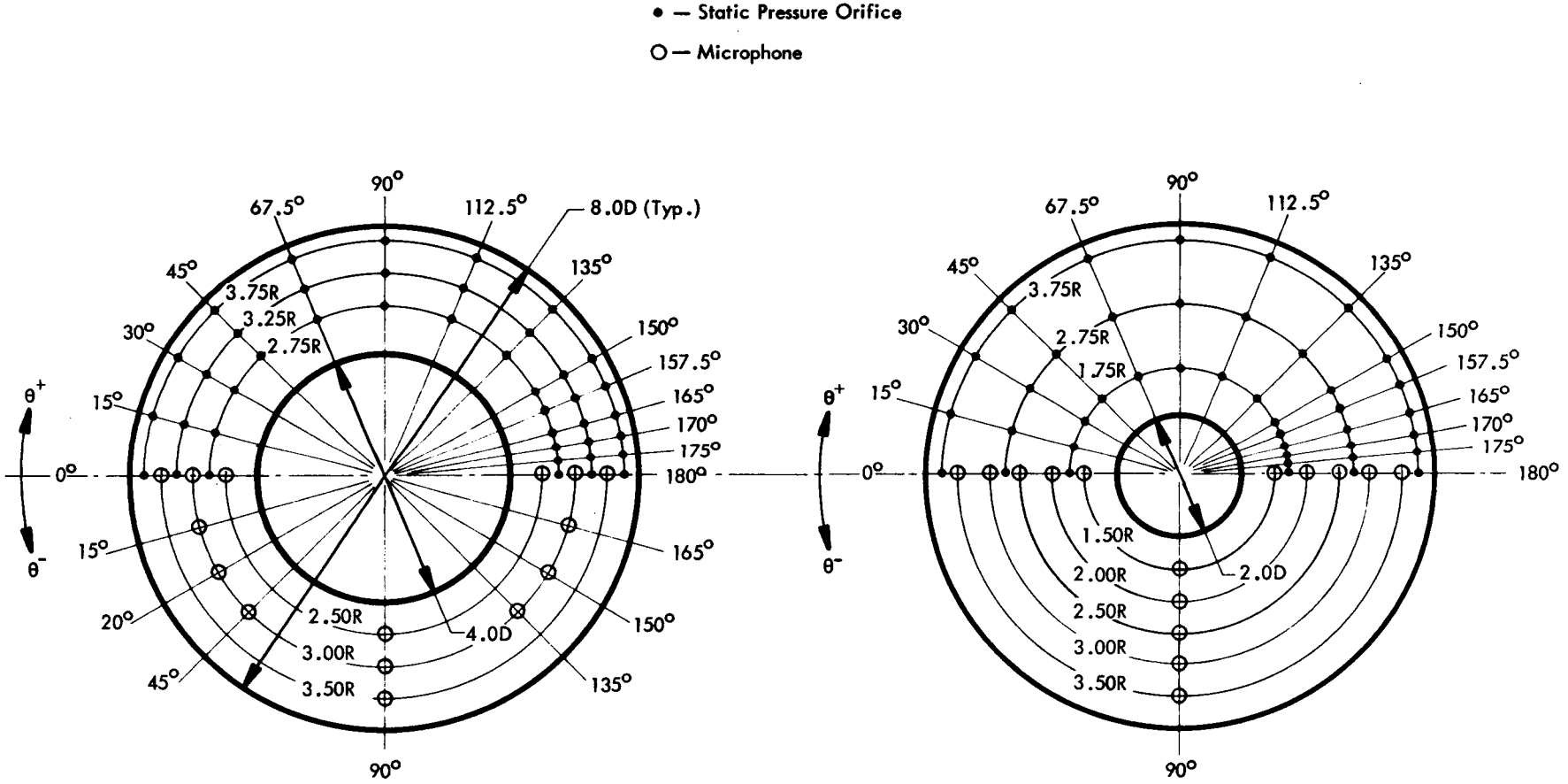

(a) Insert Plate for 4-Inch Diameter Protuberance

(b) Insert Plate for 2-Inch Diameter Protuberance

Figure 11. Instrumentation Locations in the Insert Panels

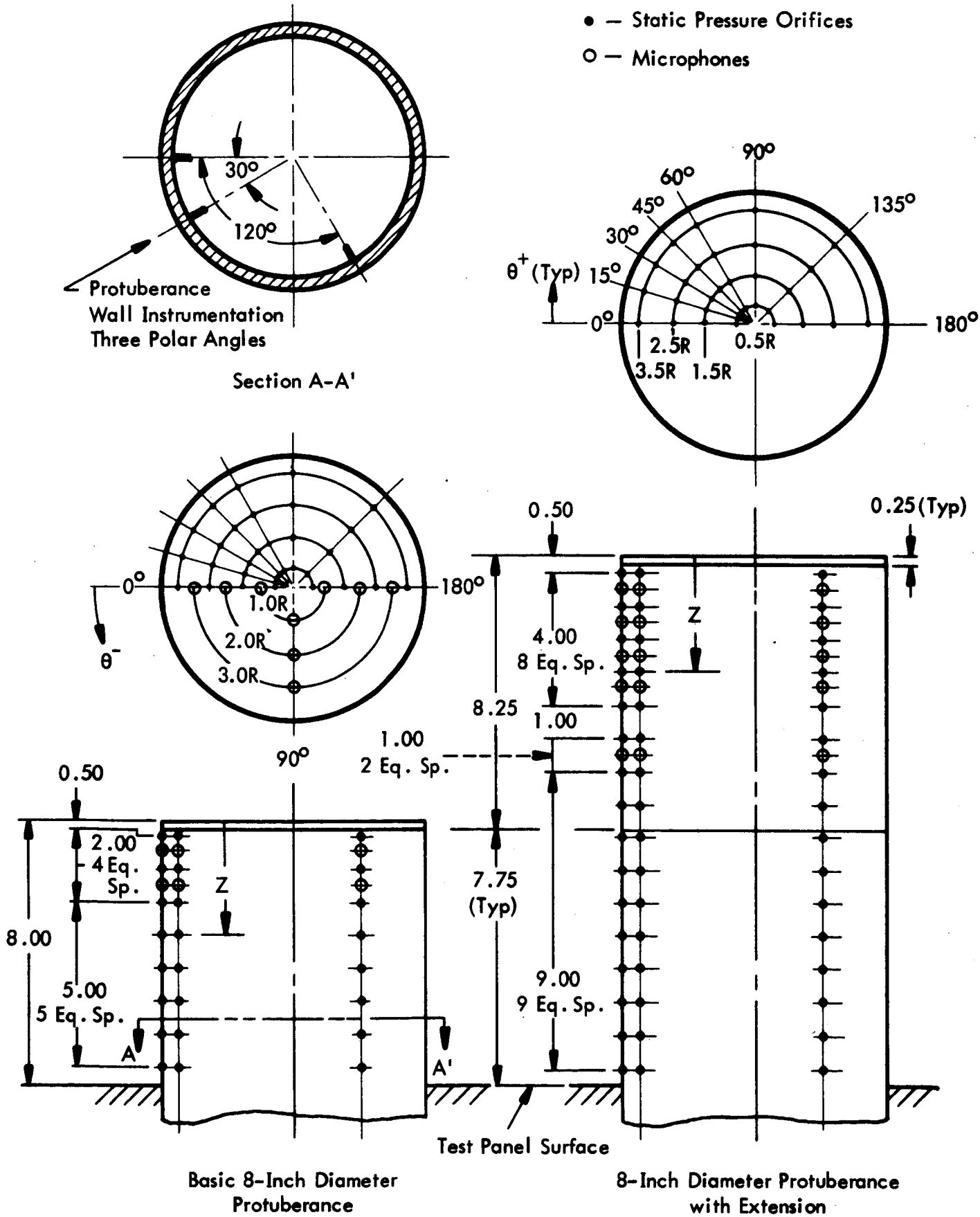

Figure 12. Instrumentation Location in the 8-Inch Diameter Protuberances.

Probe	y
1	0.029
2	0.154
3	0.279
4	0.404
5	0.529
6	0.774
7	1.029
8	1.279
9	1.529
10	1.779
11	2.029
12	2.279
13	2.539
14	2.779
15	3.029

NOTE: Linear dimensions in inches.

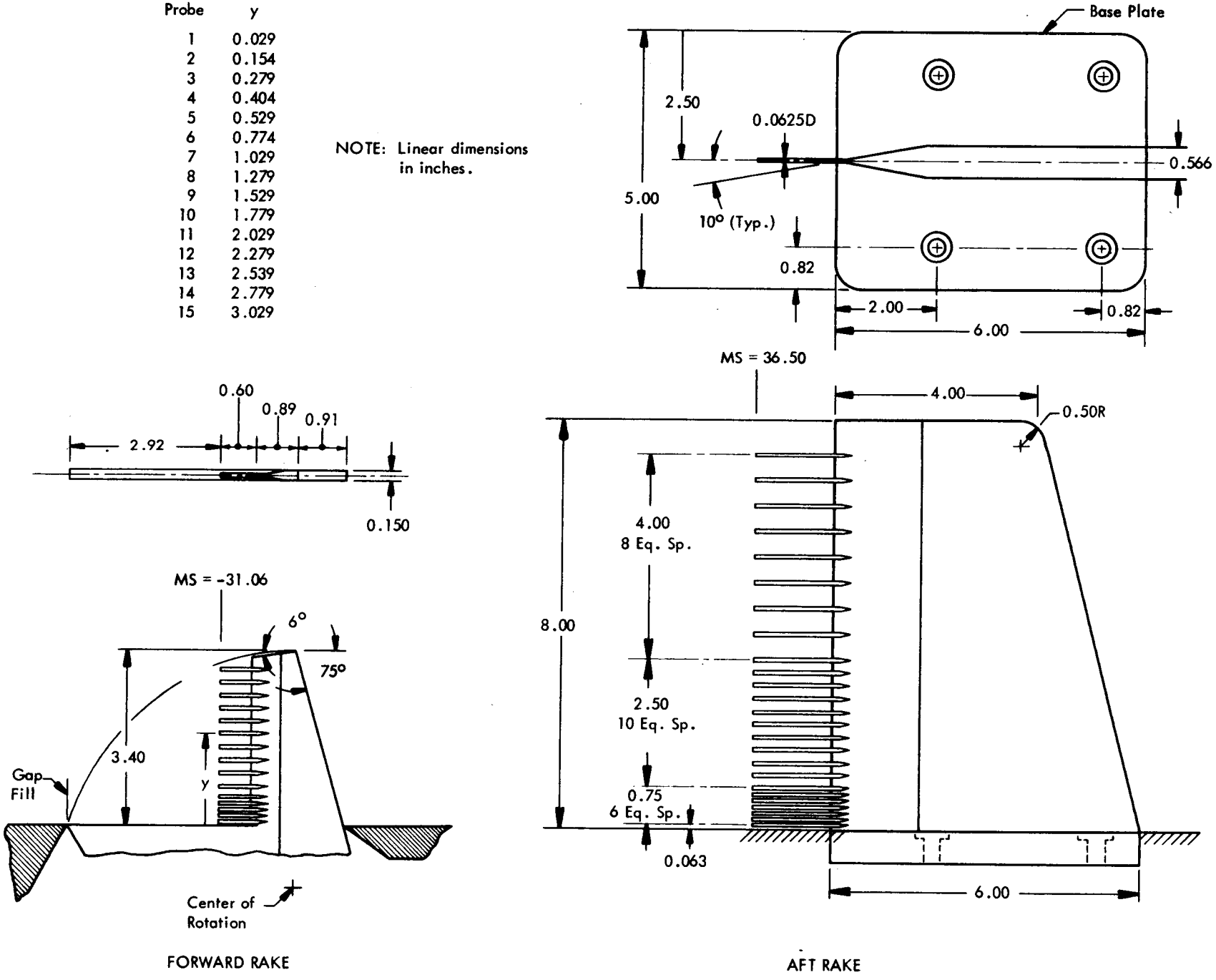

Figure 13. Details of the Boundary Layer Profile Rakes

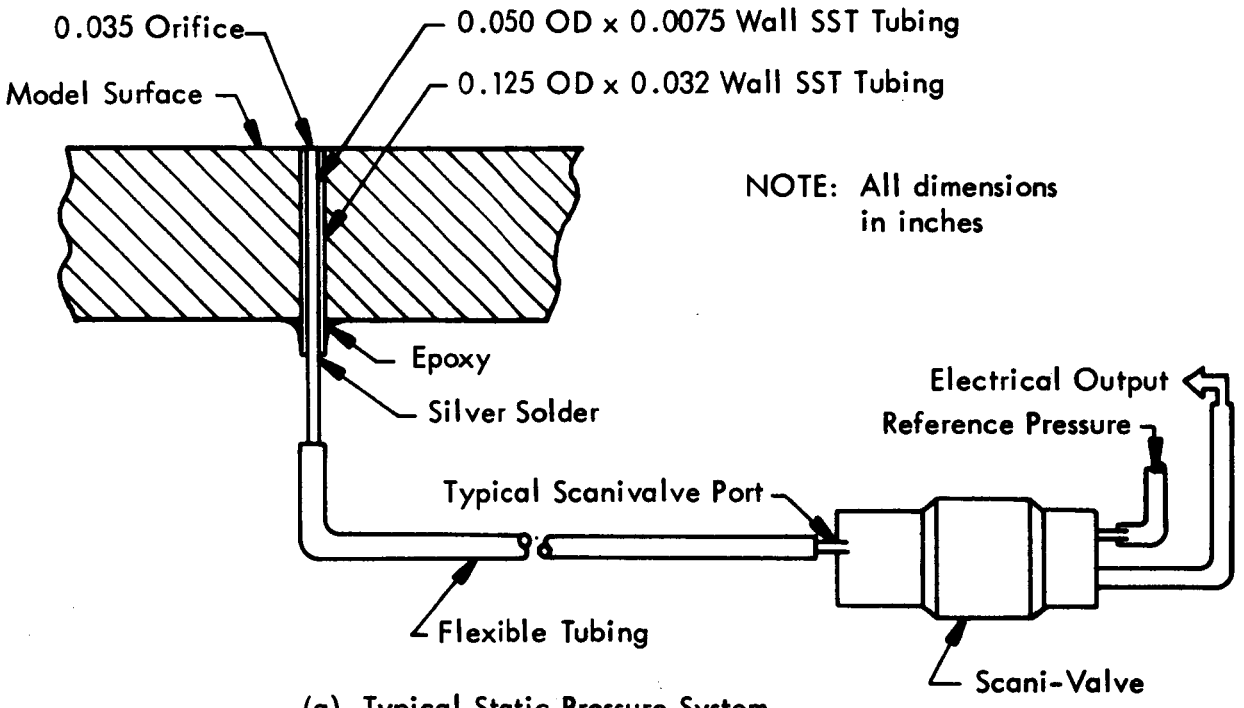

(a) Typical Static Pressure System

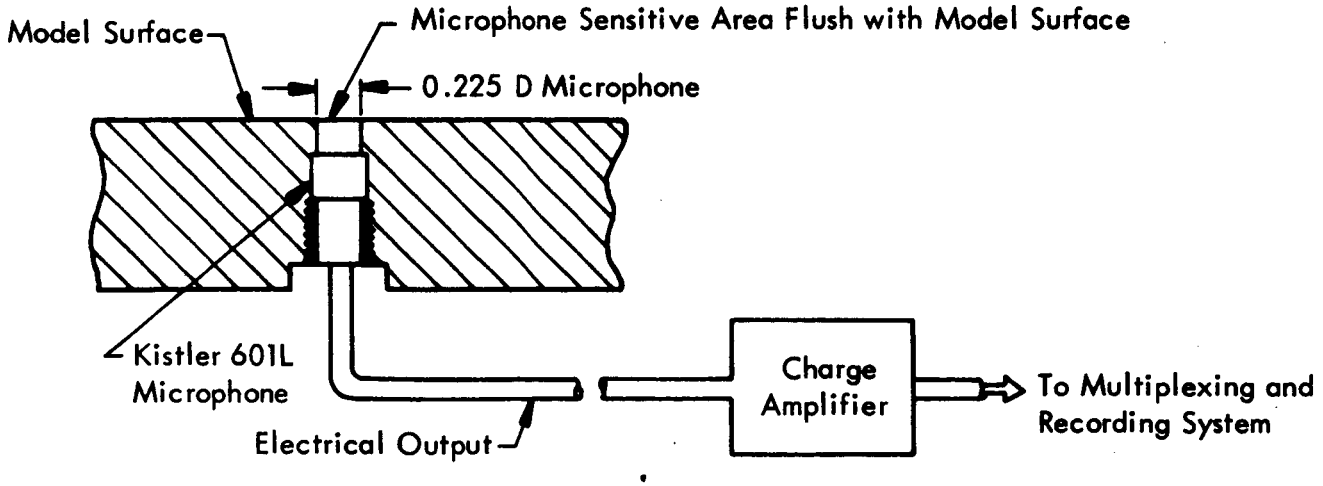

(b) Typical Microphone System

Figure 14. Details of Static Pressure and Microphone Systems

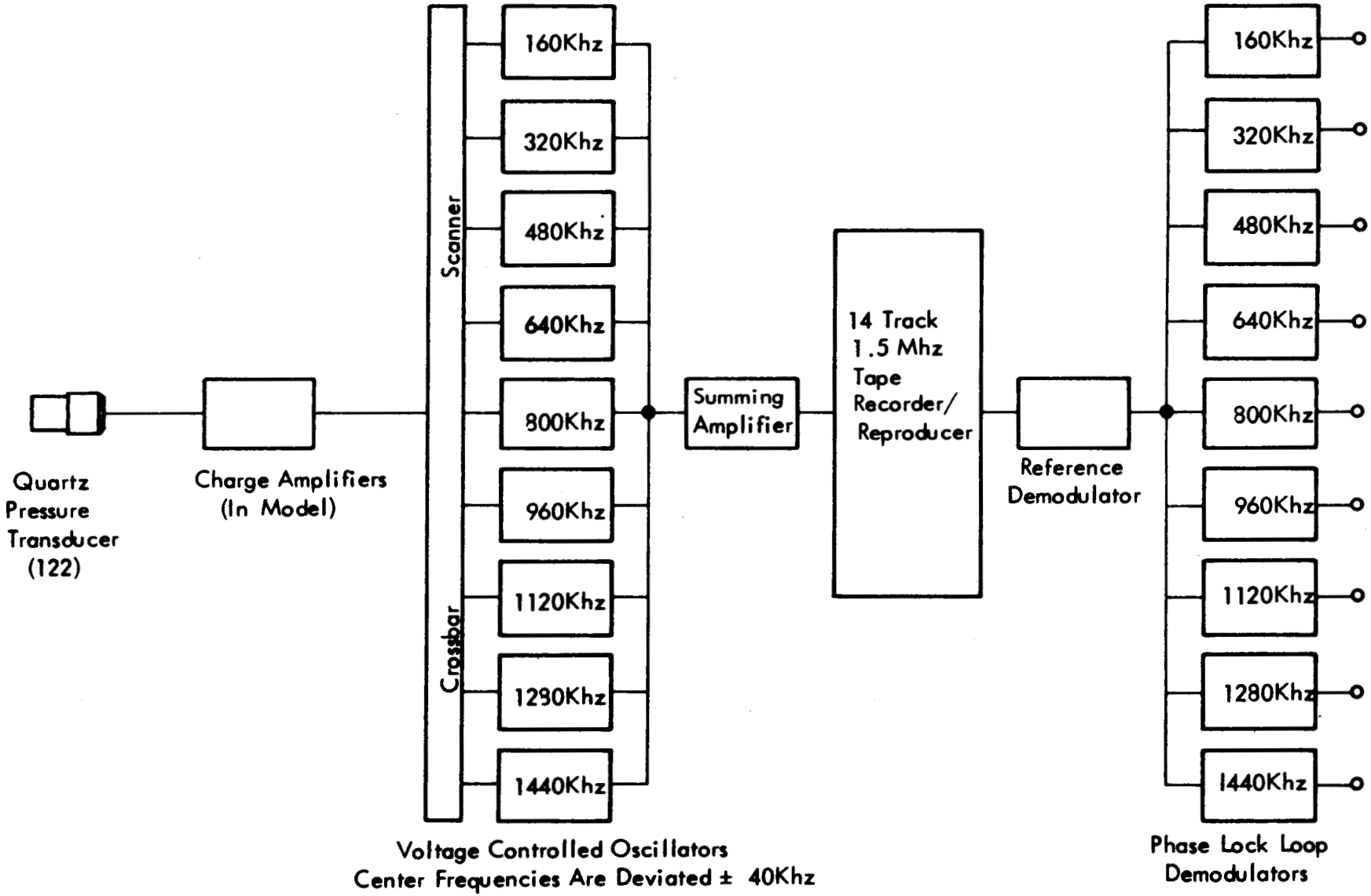

Figure 15. Block Diagram of Acoustic Recording System

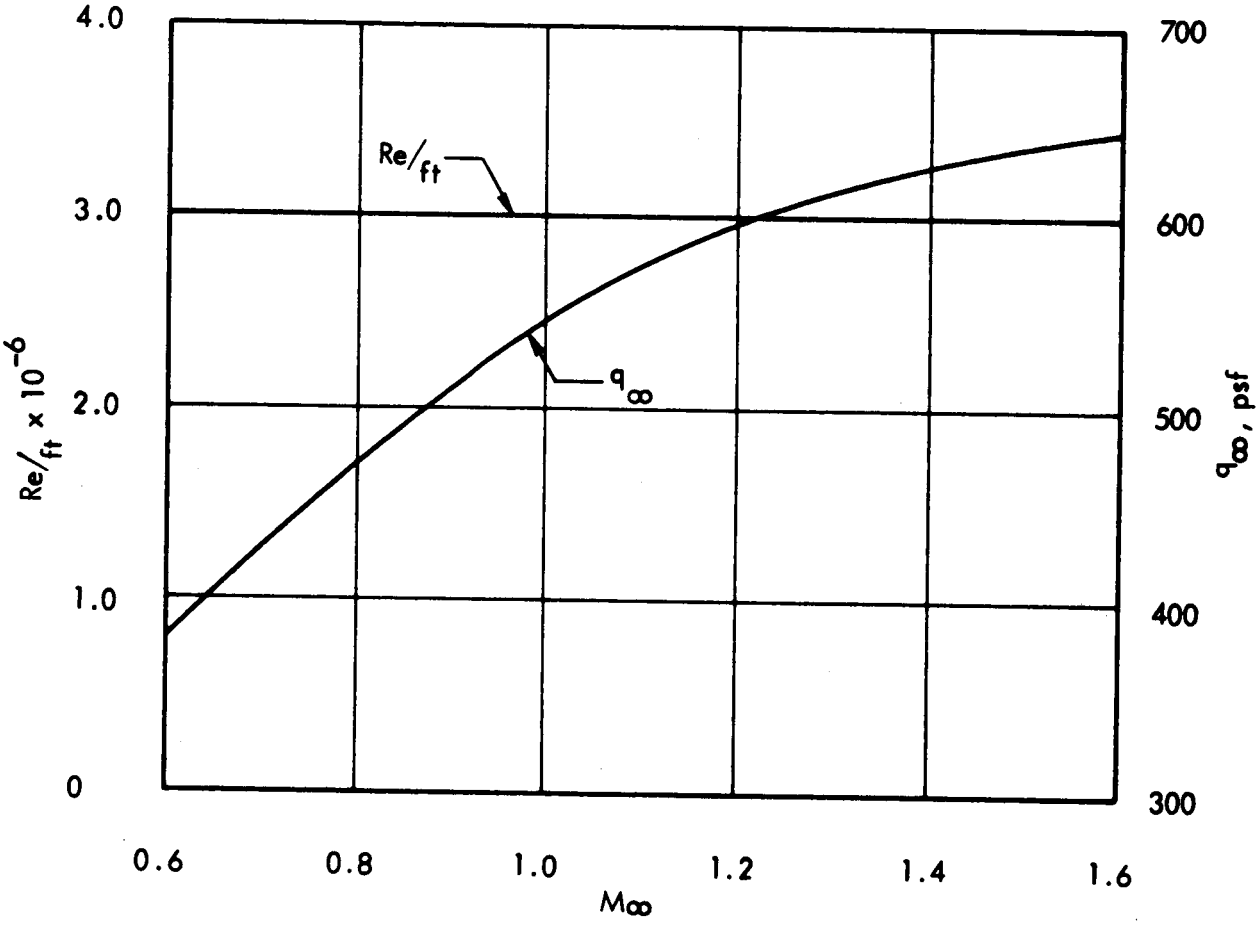

Figure 16. Variations of Unit Reynolds Number and Dynamic Pressure with Mach Number for Basic Test Conditions

TABLE I

TEST CONFIGURATIONS

Configuration Number	Description	Model Variables
1	Protuberances and Forward Boundary Layer Profile Rake Retracted	
2	Protuberances Retracted, Forward Boundary Layer Profile Rake Extended	
3	Eight-inch Diameter Protuberance with Extension, Extended	Protuberance Height, Protuberance Polar Angle
4	Basic Eight-inch Diameter Protuberance Extended	Protuberance Height, Protuberance Polar Angle
5	Four-inch Diameter Protuberance Extended	Protuberance Height
6	Two-inch Diameter Protuberance Extended	Protuberance Height
7	Reaction Control System (RCS) Protuberance Installed	
8	Auxilliary Propulsion System (APS) Protuberance Installed	
9	Boundary Layer Thickening Device, Protuberances and Forward Boundary Layer Profile Rake Retracted	
10	Boundary Layer Thickening Device, Protuberances Retracted, Forward Boundary Layer Profile Rake Extended	
11	Boundary Layer Thickening Device, Eight-inch Diameter Protuberance with Extension, Extended	Protuberance Height
12	Boundary Layer Thickening Device, Basic Eight-inch Diameter Protuberance Extended	Protuberance Height
13	Boundary Layer Thickening Device, Four-inch Diameter Protuberance Extended	Protuberance Height
14	Boundary Layer Thickening Device, Two-inch Diameter Protuberance Extended	Protuberance Height

TABLE II

PRESSURE IDENTIFICATION AND SCANI-VALVE ASSIGNMENT RECORD

Scani-Valve No. 1

	Pressure Component	Symbol	Port Number
TEST PANEL	Reference, Tunnel Total	Pta	0
	Calibrate, Tunnel Plenum	Pca	1
	$\theta^+ = 0°$; R = 26.50"	P1	2
	25.50	P2	3
	24.50	P3	4
	23.50	P4	5
	22.50	P5	6
	21.50	P6	7
	20.50	P7	8
	19.50	P8	9
	18.50	P9	10
	17.50	P10	11
	16.50	P11	12
	15.50	P12	13
	14.50	P13	14
	13.50	P14	15
	12.50	P15	16
	11.50	P16	17
	10.50	P17	18
	9.50	P18	19
	8.50	P19	20
	7.50	P20	21
	6.50	P21	22
	5.50	P22	23
	$\theta^+ = 0°$; R = 4.75"	P23	24
	$\theta^+ = 15.21°$; R = 16.52"	P24	25
	15.52	P25	26
	14.51	P26	27
	13.51	P27	28
	12.51	P28	29
	11.51	P29	30
	10.51	P30	31
	9.51	P31	32
	8.51	P32	33
	7.51	P33	34
	6.51	P34	35
	5.51	P35	36
	$\theta^+ = 15.21°$; R = 4.76"	P36	37
	Void		38 - 43
	Comparison	11P	44

Scani-Valve No. 2

	Pressure Component	Symbol	Port Number
TEST PANEL	Reference, Tunnel Total	Pta	0
	Calibrate, Tunnel Plenum	Pca	1
	$\theta^+ = 30.37°$; R = 16.56"	P37	2
	15.56	P38	3
	14.55	P39	4
	13.55	P40	5
	12.55	P41	6
	11.54	P42	7
	10.54	P43	8
	9.54	P44	9
	8.53	P45	10
	7.53	P46	11
	6.52	P47	12
	5.52	P48	13
	$\theta^+ = 30.37°$; R = 4.77"	P49	14
	$\theta^+ = 45.42°$; R = 16.62"	P50	15
	15.62	P51	16
	14.61	P52	17
	13.60	P53	18
	12.59	P54	19
	11.59	P55	20
	10.58	P56	21
	9.57	P57	22
	8.56	P58	23
	7.56	P59	24
	6.55	P60	25
	5.54	P61	26
	$\theta^+ = 45.42°$; R = 4.79"	P62	27
	$\theta^+ = 67.80°$; R = 16.74"	P63	28
	15.73	P64	29
	14.71	P65	30
	13.70	P66	31
	12.68	P67	32
	11.67	P68	33
	10.65	P69	34
	9.64	P70	35
	8.63	P71	36
	7.61	P72	37
	6.60	P73	38
	5.57	P74	39
	$\theta^+ = 67.80°$; R = 4.81"	P75	40
	Void		41 - 43
	Comparison	12P	44

TABLE II (Continued)

Scani-Valve No. 3

	Pressure Component	Symbol	Port Number
TEST PANEL	Reference, Tunnel Total	Pta	0
	Calibrate, Tunnel Plenum	Pca	1
	$\theta^+ = 90.00^\circ$; R = 16.74"	P76	2
	15.73	P77	3
	14.71	P78	4
	13.70	P79	5
	12.68	P80	6
	11.67	P81	7
	10.66	P82	8
	9.64	P83	9
	8.63	P84	10
	7.61	P85	11
	6.60	P86	12
	5.58	P87	13
	$\theta^+ = 90.00^\circ$; R = 4.82"	P88	14
	$\theta^+ = 112.21^\circ$; R = 16.71"	P89	15
	15.70	P90	16
	14.68	P91	17
	13.67	P92	18
	12.66	P93	19
	11.65	P94	20
	10.63	P95	21
	9.62	P96	22
	8.61	P97	23
	7.68	P98	24
	6.58	P99	25
	5.60	P100	26
	$\theta^+ = 112.21^\circ$; R = 4.81"	P101	27
	$\theta^+ = 134.58^\circ$; R = 16.62"	P102	28
	15.62	P103	29
	14.61	P104	30
	13.60	P105	31
	12.59	P106	32
	11.59	P107	33
	10.58	P108	34
	9.57	P109	35
	8.56	P110	36
	7.56	P111	37
	6.55	P112	38
	5.54	P113	39
	$\theta^+ = 134.58^\circ$; R = 4.79"	P114	40
	Void		41-43
	Comparison	13P	44

Scani-Valve No. 4

	Pressure Component	Symbol	Port Number
TEST PANEL	Reference, Tunnel Total	Pta	0
	Calibrate, Tunnel Plenum	Pca	1
	$\theta^+ = 149.64^\circ$; R = 16.56"	P115	2
	15.56	P116	3
	14.55	P117	4
	13.55	P118	5
	12.55	P119	6
	11.54	P120	7
	10.54	P121	8
	9.54	P122	9
	8.53	P123	10
	7.53	P124	11
	6.52	P125	12
	5.52	P126	13
	$\theta^+ = 149.64^\circ$; R = 4.77"	P127	14
	$\theta^+ = 157.20^\circ$; R = 16.54"	P128	15
	15.53	P129	16
	14.53	P130	17
	13.53	P131	18
	12.53	P132	19
	11.53	P133	20
	10.52	P134	21
	9.52	P135	22
	8.52	P136	23
	7.52	P137	24
	6.51	P138	25
	5.51	P139	26
	$\theta^+ = 157.20^\circ$; R = 4.76"	P140	27
	$\theta^+ = 164.79^\circ$; R = 16.52"	P141	28
	15.52	P142	29
	14.51	P143	30
	13.51	P144	31
	12.51	P145	32
	11.51	P146	33
	10.51	P147	34
	9.51	P148	35
	8.51	P149	36
	7.51	P150	37
	6.51	P151	38
	5.51	P152	39
	$\theta^+ = 164.79^\circ$; R = 4.76"	P153	40
	Void		41-43
	Comparison	14P	44

TABLE II (Continued)

Scani-Valve No. 5

	Pressure Component	Symbol	Port Number
TEST PANEL	Reference, Tunnel Total	Pta	0
	Calibrate, Tunnel Plenum	Pca	1
	$\theta^+ = 169.86^\circ$; R = 16.51"	P154	2
	15.51	P155	3
	14.51	P156	4
	13.51	P157	5
	12.51	P158	6
	11.51	P159	7
	10.51	P160	8
	9.50	P161	9
	8.50	P162	10
	7.50	P163	11
	6.50	P164	12
	5.50	P165	13
	$\theta^+ = 169.86^\circ$; R = 4.75"	P166	14
	$\theta^+ = 174.93^\circ$; R = 16.51"	P167	15
	15.51	P168	16
	14.51	P169	17
	13.51	P170	18
	12.51	P171	19
	11.51	P172	20
	10.51	P173	21
	9.50	P174	22
	8.50	P175	23
	7.50	P176	24
	6.50	P177	25
	5.50	P178	26
	$\theta^+ = 174.93^\circ$; R = 4.75"	P179	27
	$\theta^+ = 270.00^\circ$; R = 16.50"	P180	28
	15.50	P181	29
	14.50	P182	30
	13.50	P183	31
	12.50	P184	32
	11.50	P185	33
	10.50	P186	34
	9.50	P187	35
	8.50	P188	36
	7.50	P189	37
	6.50	P190	38
	5.50	P191	39
	$\theta^+ = 270.00^\circ$; R = 4.75"	P192	40
	Void		41-43
	Comparison	15P	44

Scani-Valve No. 6

	Pressure Component	Symbol	Port Number
FORWARD RAKE	Reference, Tunnel Total	Pta	0
	Calibrate, Tunnel Plenum	Pca	1
	Y = 0.029"	PF1	2
	0.154	PF2	3
	0.279	PF3	4
	0.404	PF4	5
	0.529	PF5	6
	0.774	PF6	7
	1.029	PF7	8
	1.279	PF8	9
	1.529	PF9	10
	1.779	PF10	11
	2.029	PF11	12
	2.279	PF12	13
	2.539	PF13	14
	2.779	PF14	15
	Y = 3.029"	PF15	16
TEST PANEL	$\theta^+ = 180.00^\circ$; R = 28.00"	P193	17
	26.50	P194	18
	25.50	P195	19
	24.50	P196	20
	23.50	P197	21
	22.50	P198	22
	21.50	P199	23
	20.50	P200	24
	19.50	P201	25
	18.50	P202	26
	17.50	P203	27
	16.50	P204	28
	15.50	P205	29
	14.50	P206	30
	13.50	P207	31
	12.50	P208	32
	11.50	P209	33
	10.50	P210	34
	9.50	P211	35
	8.50	P212	36
	7.50	P213	37
	6.50	P214	38
	5.50	P215	39
	$\theta^+ = 180.00^\circ$; R = 4.75"	P216	40
	Void		41-43
	Comparison	16P	44

TABLE II (Continued)

Scani-Valve No. 7

	Pressure Component	Symbol	Port Number
BASIC 8-INCH DIAMETER PROTUBERANCE WALL	Reference, Tunnel Total	Pta	0
	Calibrate, Tunnel Plenum	Pca	1
	0° Ray, Z = 7.50"	P249	2
	6.50	P250	3
	5.50	P251	4
	4.50	P252	5
	3.50	P253	6
	2.50	P254	7
	1.50	P255	8
	0° Ray, Z = 0.50"	P256	9
	30° Ray, Z = 7.50"	P257	10
	6.50	P258	11
	5.50	P259	12
	4.50	P260	13
	3.50	P261	14
	2.50	P262	15
	1.50	P263	16
	30° Ray, Z = 0.50"	P264	17
	120° Ray, Z = 7.50"	P265	18
	6.50	P266	19
	5.50	P267	20
	4.50	P268	21
	3.50	P269	22
	2.50	P270	23
	1.50	P271	24
	120° Ray, Z = 0.50"	P272	25
PROTUBERANCE EXTENSION	0° Ray, Z = 7.50"	P273	26
	6.50	P274	27
	5.50	P275	28
	4.50	P276	29
	3.50	P277	30
	2.50	P278	31
	1.50	P279	32
	0° Ray, Z = 0.50"	P280	33
	30° Ray, Z = 7.50"	P281	34
	6.50	P282	35
	5.50	P283	36
	4.50	P284	37
	3.50	P285	38
	2.50	P286	39
	1.50	P287	40
	30° Ray, Z = 0.50"	P288	41
	Void		42,43
	Comparison	17P	44

Scani-Valve No. 8

	Pressure Component	Symbol	Port Number
8-INCH DIAMETER PROTUBERANCE CAP	Reference, Tunnel Total	Pta	0
	Calibrate Tunnel Plenum	Pca	1
	$\theta^+ = 00.00°$; R = 3.50"	P217	2
	2.50	P218	3
	1.50	P219	4
	$\theta^+ = 00.00°$; R = 0.50"	P220	5
	$\theta^+ = 15.00°$; R = 3.50"	P221	6
	2.50	P222	7
	1.50	P223	8
	$\theta^+ = 15.00°$; R = 0.50"	P224	9
	$\theta^+ = 30.00°$; R = 3.50"	P225	10
	2.50	P226	11
	1.50	P227	12
	$\theta^+ = 30.00°$; R = 0.50"	P228	13
	$\theta^+ = 45.00°$; R = 3.50"	P229	14
	2.50	P230	15
	1.50	P231	16
	$\theta^+ = 45.00°$; R = 0.50"	P232	17
	$\theta^+ = 60.00°$; R = 3.50"	P233	18
	2.50	P234	19
	1.50	P235	20
	$\theta^+ = 60.00°$; R = 0.50"	P236	21
	$\theta^+ = 90.00°$; R = 3.50"	P237	22
	2.50	P238	23
	1.50	P239	24
	$\theta^+ = 90.00°$; R = 0.50"	P240	25
	$\theta^+ = 135.00°$; R = 3.50"	P241	26
	2.50	P242	27
	1.50	P243	28
	$\theta^+ = 135.00°$; R = 0.50"	P244	29
	$\theta^+ = 180.00°$; R = 3.50"	P245	30
	2.50	P246	31
	1.50	P247	32
	$\theta^+ = 180.00°$; R = 0.50"	P248	33
PROTUBERANCE EXTENSION	120° Ray, Z = 7.50"	P289	34
	6.50	P290	35
	5.50	P291	36
	4.50	P292	37
	3.50	P293	38
	2.50	P294	39
	1.50	P295	40
	120° Ray, Z = 0.50"	P296	41
	Void		42,43
	Comparison	18P	44

TABLE II (Concluded)

Scani-Valve No. 9

	Pressure Component	Symbol	Port Number
4-INCH DIAMETER PROTUBERANCE INSERT PANEL	Reference, Tunnel Total	Pta	0
	Calibrate, Tunnel Plenum	Pca	1
	$\theta^+ = 00.00^\circ$; R = 3.75"	P297	2
	3.25	P298	3
	$\theta^+ = 00.00^\circ$; R = 2.75"	P299	4
	$\theta^+ = 15.00^\circ$; R = 3.75"	P300	5
	3.25	P301	6
	$\theta^+ = 15.00^\circ$; R = 2.75"	P302	7
	$\theta^+ = 30.00^\circ$; R = 3.75"	P303	8
	3.25	P304	9
	$\theta^+ = 30.00^\circ$; R = 2.75"	P305	10
	$\theta^+ = 45.00^\circ$; R = 3.75"	P306	11
	3.25	P307	12
	$\theta^+ = 45.00^\circ$; R = 2.75"	P308	13
	$\theta^+ = 67.50^\circ$; R = 3.75"	P309	14
	3.25	P310	15
	$\theta^+ = 67.50^\circ$; R = 2.75"	P311	16
	$\theta^+ = 90.00^\circ$; R = 3.75"	P312	17
	3.25	P313	18
	$\theta^+ = 90.00^\circ$; R = 2.75"	P314	19
	$\theta^+ = 112.50^\circ$; R = 3.75"	P315	20
	3.25	P316	21
	$\theta^+ = 112.50^\circ$; R = 2.75"	P317	22
	$\theta^+ = 135.00^\circ$; R = 3.75"	P318	23
	3.25	P319	24
	$\theta^+ = 135.00^\circ$; R = 2.75"	P320	25
	$\theta^+ = 150.00^\circ$; R = 3.75"	P321	26
	3.25	P322	27
	$\theta^+ = 150.00^\circ$; R = 2.75"	P323	28
	$\theta^+ = 157.50^\circ$; R = 3.75"	P324	29
	3.25	P325	30
	$\theta^+ = 157.50^\circ$; R = 2.75"	P326	31
	$\theta^+ = 165.00^\circ$; R = 3.75"	P327	32
	3.25	P328	33
	$\theta^+ = 165.00^\circ$; R = 2.75"	P329	34
	$\theta^+ = 170.00^\circ$; R = 3.75"	P330	35
	3.25	P331	36
	$\theta^+ = 170.00^\circ$; R = 2.75"	P332	37
	$\theta^+ = 175.00^\circ$; R = 3.75"	P333	38
	3.25	P334	39
	$\theta^+ = 175.00^\circ$; R = 2.75"	P335	40
	$\theta^+ = 180.00^\circ$; R = 3.75"	P336	41
	3.25	P337	42
	$\theta^+ = 180.00^\circ$; R = 2.75"	P338	43
	Comparison	19P	44

Scani-Valve No. 10

	Pressure Component	Symbol	Port Number
2-INCH DIAMETER PROTUBERANCE INSERT PANEL	Reference, Tunnel Total	Pta	0
	Calibrate, Tunnel Plenum	Pca	1
	$\theta^+ = 00.00^\circ$; R = 3.75"	P339	2
	2.75	P340	3
	$\theta^+ = 00.00^\circ$; R = 1.75"	P341	4
	$\theta^+ = 15.00^\circ$; R = 3.75"	P342	5
	2.75	P343	6
	$\theta^+ = 15.00^\circ$; R = 1.75"	P344	7
	$\theta^+ = 30.00^\circ$; R = 3.75"	P345	8
	2.75	P346	9
	$\theta^+ = 30.00^\circ$; R = 1.75"	P347	10
	$\theta^+ = 45.00^\circ$; R = 3.75"	P348	11
	2.75	P349	12
	$\theta^+ = 45.00^\circ$; R = 1.75"	P350	13
	$\theta^+ = 67.50^\circ$; R = 3.75"	P351	14
	2.75	P352	15
	$\theta^+ = 67.50^\circ$; R = 1.75"	P353	16
	$\theta^+ = 90.00^\circ$; R = 3.75"	P354	17
	2.75	P355	18
	$\theta^+ = 90.00^\circ$; R = 1.75"	P356	19
	$\theta^+ = 112.50^\circ$; R = 3.75"	P357	20
	2.75	P358	21
	$\theta^+ = 112.50^\circ$; R = 1.75"	P359	22
	$\theta^+ = 135.00^\circ$; R = 3.75"	P360	23
	2.75	P361	24
	$\theta^+ = 135.00^\circ$; R = 1.75"	P362	25
	$\theta^+ = 150.00^\circ$; R = 3.75"	P363	26
	2.75	P364	27
	$\theta^+ = 150.00^\circ$; R = 1.75"	P365	28
	$\theta^+ = 157.50^\circ$; R = 3.75"	P366	29
	2.75	P367	30
	$\theta^+ = 157.50^\circ$; R = 1.75"	P368	31
	$\theta^+ = 165.00^\circ$; R = 3.75"	P369	32
	2.75	P370	33
	$\theta^+ = 165.00^\circ$; R = 1.75"	P371	34
	$\theta^+ = 170.00^\circ$; R = 3.75"	P372	35
	2.75	P373	36
	$\theta^+ = 170.00^\circ$; R = 1.75"	P374	37
	$\theta^+ = 175.00^\circ$; R = 3.75"	P375	38
	2.75	P376	39
	$\theta^+ = 175.00^\circ$; R = 1.75"	P377	40
	$\theta^+ = 180.00^\circ$; R = 3.75"	P378	41
	2.75	P379	42
	$\theta^+ = 180.00^\circ$; R = 1.75"	P380	43
	Comparison	110P	44

TABLE III

PRESSURE IDENTIFICATION RECORD FOR AFT BOUNDARY LAYER PROFILE RAKE

P^2B Channel	Pitot Probe Location	Symbol	Reference Pressure
1	y = 0.063	PA1	Pca
2	y = 0.188	PA2	
3	y = 0.313	PA3	
4	y = 0.438	PA4	
5	y = 0.563	PA5	
6	y = 0.688	PA6	
7	y = 0.813	PA7	
8	y = 1.063	PA8	
9	y = 1.313	PA9	
10	y = 1.563	PA10	
11	y = 1.813	PA11	
12	y = 1.063	PA12	
13	y = 2.313	PA13	
14	y = 2.563	PA14	
15	y = 2.813	PA15	
16	y = 3.063	PA16	
17	y = 3.313	PA17	
18	y = 3.813	PA18	
19	y = 4.313	PA19	
20	y = 4.813	PA20	
21	y = 5.313	PA21	
22	y = 5.813	PA22	
23	y = 6.313	PA23	
24	y = 6.813	PA24	
25	y = 7.313	PA25	

TABLE IV

MICROPHONE IDENTIFICATION AND TAPE TRACK ASSIGNMENT RECORD

Tape Track No. 1

	Microphone Component	Symbol	Center Frequency
TEST PANEL	$\theta^- = 00.00^\circ$; R = 15.00"	M5	160 Khz
	14.00	M6	320
	13.00	M7	480
	12.00	M8	640
	11.00	M9	800
	10.00	M10	960
	9.00	M11	1120
	8.00	M12	1280
	$\theta^- = 00.00^\circ$; R = 7.00"	M13	1440 Khz

Tape Track No. 2

	Microphone Component	Symbol	Center Frequency
TEST PANEL	$\theta^- = 15.00^\circ$; R = 16.00"	M16	160 Khz
	14.00	M17	320
	12.00	M18	480
	10.00	M19	640
	8.00	M20	800
	7.00	M21	960
	6.00	M22	1120
	$\theta^- = 15.00^\circ$; R = 5.00"	M23	1280
	$\theta^- = 67.50^\circ$; R = 16.00"	M40	1440Khz

Tape Track No. 3

	Microphone Component	Symbol	Center Frequency
TEST PANEL	$\theta^- = 30.00^\circ$; R = 16.00"	M24	160 Khz
	14.00	M25	320
	12.00	M26	480
	10.00	M27	640
	8.00	M28	800
	7.00	M29	960
	6.00	M30	1120
	$\theta^- = 30.00^\circ$; R = 5.00"	M31	1280
	$\theta^- = 67.50^\circ$; R = 14.00"	M41	1440 Khz

Tape Track No. 4

	Microphone Component	Symbol	Center Frequency
TEST PANEL	$\theta^- = 45.00^\circ$; R = 16.00"	M32	160 Khz
	14.00	M33	320
	12.00	M34	480
	10.00	M35	640
	8.00	M36	800
	7.00	M37	960
	6.00	M38	1120
	$\theta^- = 45.00^\circ$; R = 5.00"	M39	1280
	$\theta^- = 67.50^\circ$; R = 12.00"	M42	1440 Khz

Tape Track No. 5

	Microphone Component	Symbol	Center Frequency
TEST PANEL	$\theta^- = 90.00^\circ$; R = 16.00"	M48	160 Khz
	14.00	M49	320
	12.00	M50	480
	10.00	M51	640
	8.00	M52	800
	7.00	M53	960
	6.00	M54	1120
	$\theta^- = 90.00^\circ$; R = 5.00"	M55	1280
	$\theta^- = 67.50^\circ$; R = 10.00"	M43	1440 Khz

Tape Track No. 6

	Microphone Component	Symbol	Center Frequency
TEST PANEL	$\theta^- = 135.00^\circ$; R = 16.00"	M56	160 Khz
	14.00	M57	320
	12.00	M58	480
	10.00	M59	640
	8.00	M60	800
	7.00	M61	960
	6.00	M62	1120
	$\theta^- = 135.00^\circ$; R = 5.00"	M63	1280
	$\theta^- = 67.50^\circ$; R = 8.00"	M44	1440 Khz

Tape Track No. 7

	Microphone Component	Symbol	Center Frequency
TEST PANEL	Voice and Time Code	VT	32 Khz
	$\theta^- = 00.00^\circ$; R = 20.00"	M1	160
	18.00	M2	320
	17.00	M3	480
	$\theta^- = 00.00^\circ$; R = 16.00"	M4	640
	$\theta^- = 67.50^\circ$; R = 7.00"	M45	800
	6.00	M46	960
	$\theta^- = 67.50^\circ$; R = 5.00"	M47	1120
	Void		1280
	Reference	R	1440 Khz

Tape Track No. 8

	Microphone Component	Symbol	Center Frequency
T.P.	Voice and Time Code	VT	32 Khz
	$\theta^- = 00.00^\circ$; R = 6.00"	M14	160
	$\theta^- = 00.00^\circ$; R = 5.00"	M15	320
	Depends on Configurations	M108	480
	See Table V	M109	640
		M110	800
		M111	960
		M112	1120
	Void		1280
	Reference	R	1440 Khz

TABLE IV (Concluded)

Tape Track No. 9

	Microphone Component	Symbol	Center Frequency
TEST PANEL	$\theta^- = 165.00^\circ$; R = 16.00"	M72	160 Khz
	14.00	M73	320
	12.00	M74	480
	10.00	M75	640
	8.00	M76	800
	7.00	M77	960
	6.00	M78	1120
	$\theta^- = 165.00^\circ$; R = 5.00"	M79	1280
	$\theta^- = 150.00^\circ$; R = 16.00"	M64	1440 Khz

Tape Track No. 10

	Microphone Component	Symbol	Center Frequency
TEST PANEL	$\theta^- = 170.00^\circ$; R = 16.00"	M80	160 Khz
	14.00	M81	320
	12.00	M82	480
	10.00	M83	640
	8.00	M84	800
	7.00	M85	960
	6.00	M86	1120
	$\theta^- = 170.00^\circ$; R = 5.00"	M87	1280
	$\theta^- = 150.00^\circ$; R = 14.00"	M65	1440 Khz

Tape Track No. 11

	Microphone Component	Symbol	Center Frequency
TEST PANEL	$\theta^- = 175.00^\circ$; R = 16.00"	M88	160 Khz
	14.00	M89	320
	12.00	M90	480
	10.00	M91	640
	8.00	M92	800
	7.00	M93	960
	6.00	M94	1120
	$\theta^- = 175.00^\circ$; R = 5.00"	M95	1280
	$\theta^- = 150.00^\circ$; R = 12.00"	M66	1440 Khz

Tape Track No. 12

	Microphone Component	Symbol	Center Frequency
TEST PANEL	$\theta^- = 180.00^\circ$; R = 13.00"	M99	160 Khz
	12.00	M100	320
	11.00	M101	480
	10.00	M102	640
	9.00	M103	800
	8.00	M104	960
	7.00	M105	1120
	6.00	M106	1280
	$\theta^- = 180.00^\circ$; R = 5.00"	M107	1440 Khz

Tape Track No. 13

	Microphone Component	Symbol	Center Frequency
TEST PANEL	$\theta^- = 180.00^\circ$; R = 20.00"	M96	160 Khz
	16.00	M97	320
	$\theta^- = 180.00^\circ$; R = 14.00"	M98	480
	Depends on Configurations	M113	640
	See Table V	M114	800
		M115	960
		M116	1120
		M117	1280
T.P.	$\theta^- = 150.00^\circ$; R = 10.00"	M67	1440 Khz

Tape Track No. 14

	Microphone Component	Symbol	Center Frequency
	Depends on Configurations	M118	160 Khz
	See Table V	M119	320
		M120	480
		M121	640
		M122	800
TEST PANEL	$\theta^- = 150.00^\circ$; R = 8.00"	M68	960
	7.00	M69	1120
	6.00	M70	1280
	$\theta^- = 150.00^\circ$; R = 25.00"	M71	1440 Khz

TABLE V

MICROPHONE IDENTIFICATION RECORD FOR INSERT PANELS AND 8-INCH DIAMETER PROTUBERANCES

2-Inch Diameter Protuberance Insert Panel

Microphone	Location
M108	$\theta^- = 00.00^\circ$; R = 3.50"
M109	3.00
M110	2.50
M111	2.00
M112	$\theta^- = 00.00^\circ$; R = 1.50"
M113	$\theta^- = 90.00^\circ$; R = 3.50"
M114	3.00
M115	2.50
M116	2.00
M117	$\theta^- = 90.00^\circ$; R = 1.50"
M118	$\theta^- = 180.00^\circ$; R = 3.50"
M119	3.00
M120	2.00
M121	2.00
M122	$\theta^- = 180.00^\circ$; R = 1.50"

4-Inch Diameter Protuberance Insert Panel

Microphone	Location
M108	$\theta^- = 00.00^\circ$; R = 3.50"
M109	3.00
M110	$\theta^- = 00.00^\circ$; R = 2.50"
M111	$\theta^- = 15.00^\circ$; R = 3.00"
M112	$\theta^- = 30.00^\circ$; R = 3.00"
M113	$\theta^- = 45.00^\circ$; R = 3.00"
M114	$\theta^- = 90.00^\circ$; R = 3.50"
M115	3.00
M116	$\theta^- = 90.00^\circ$; R = 2.50"
M117	$\theta^- = 135.00^\circ$; R = 3.00"
M118	$\theta^- = 150.00^\circ$; R = 3.00"
M119	$\theta^- = 165.00^\circ$; R = 3.00"
M120	$\theta^- = 180.00^\circ$; R = 3.50"
M121	3.00
M122	$\theta^- = 180.00^\circ$; R = 2.50"

Basic 8-Inch Diameter Protuberance

Microphone		Location	
M108	WALL	0° Ray,	Z = 2.00"
M109		0° Ray,	Z = 1.00"
M110		30° Ray,	Z = 2.00"
M111		30° Ray,	Z = 1.00"
M112		120° Ray,	Z = 2.00"
M113		120° Ray,	Z = 1.00"
M114	CAP	$\theta^- = 00.00^\circ$;	R = 3.00"
M115		2.00	
M116		$\theta^- = 00.00^\circ$;	R = 1.00"
M117		$\theta^- = 90.00^\circ$;	R = 3.00"
M118		2.00	
M119		$\theta^- = 90.00^\circ$;	R = 1.00"
M120		$\theta^- = 180.00^\circ$;	R = 3.00"
M121		2.00	
M122		$\theta^- = 180.00^\circ$;	R = 1.00"

8-Inch Diameter Protuberance Extension

Microphone		Location	
M108	WALL	0° Ray,	Z = 6.00"
M109		4.00	
M110		3.00	
M111		2.00	
M112		0° Ray,	Z = 1.00"
M113		30° Ray,	Z = 6.00"
M114		4.00	
M115		3.00	
M116		2.00	
M117		30° Ray,	Z = 1.00"
M118		120° Ray,	Z = 6.00"
M119		4.00	
M120		3.00	
M121		2.00	
M122		120° Ray,	Z = 1.00"

TABLE VI

TENTATIVE RUN SCHEDULE

Run Sequence	Configuration Number	M_∞ Range	Re/ft x 10^6	H/D	Protuberance Polar Angle	Test Procedure
1	1	0.6 - 1.6	3.0	-	-	-
2	1	↓	1.5	-	-	-
3	1	↓	4.5	-	-	-
4	2	↓	3.0	-	-	-
5	3	↓	↓	1.0 - 2.0	0°	*
6	3	↓	↓	↓	15°	*
7	3	↓	↓	↓	60°	*
8	3	↓	1.5	↓	0°	*
9	3	↓	4.5	↓	0°	*
10	4	↓	3.0	0 - 1.0	↓	*
11	4	↓	↓	↓	15°	*
12	4	↓	↓	↓	60°	*
13	4	↓	1.5	↓	0°	*
14	4	↓	4.5	↓	↓	*
15	5	↓	3.0	0 - 2.0	↓	*
16	5	↓	1.5	↓	↓	*
17	5	↓	4.5	↓	↓	*
18	6	↓	3.0	0 - 4.0	↓	*
19	6	↓	1.5	↓	↓	*
20	6	↓	4.5	↓	↓	*
21	7	↓	3.0	-	-	-
22	8	↓	↓	-	-	-
23	9	↓	↓	-	-	-
24	10	↓	↓	-	-	-
25	11	↓	↓	1.0 - 2.0	0°	*
26	12	↓	↓	0 - 1.0	↓	*
27	13	↓	↓	0 - 2.0	↓	*
28	14	↓	↓	0 - 4.0	↓	*

* Protuberance height will be varied holding Mach number constant.